GUIDE FOR THE

ASSESSMENT OF PARAMETRIC ROLL RESONANCE IN THE DESIGN OF CONTAINER CARRIERS

SEPTEMBER 2004 (Updated June 2008 – see next page)

American Bureau of Shipping
Incorporated by Act of Legislature of
the State of New York 1862

Updates

June 2008 consolidation includes:

- September version plus Notice No. 1, Corrigenda/Editorials

Foreword

The main purpose of this Guide is to supplement the Rules and the other design and analysis criteria that ABS issues for the classification of container carriers in relation to parametric roll resonance phenomenon.

The Guide contains a brief description of the physical phenomenon of parametric roll resonance, which may cause an excessive roll of a containership in longitudinal (head and following) waves. The Guide also contains a description of criteria used to determine if a particular vessel is vulnerable to parametric roll (susceptibility criteria) and how large these roll motions might be (severity criteria). Recommendations are given for further actions if a ship is found to be endangered by the possibility of parametric roll, including numerical simulations and a model test. Means of mitigation of consequences of the parametric roll are briefly considered.

If criteria and requirements included in this Guide are satisfied, ABS may assign an optional class notation as recognition of safety performance in relation to parametric roll resonance.

ABS welcomes comments and suggestions for improvement of this Guide. *Comments or suggestions can be sent electronically to rdd@eagle.org*.

This Page Intentionally Left Blank

GUIDE FOR THE

ASSESSMENT OF PARAMETRIC ROLL RESONANCE IN THE DESIGN OF CONTAINER CARRIERS

CONTENTS

This Page Intentionally Left Blank

SECTION **1 Introduction**

1 Parametric Roll Resonance in Longitudinal Waves

1.1 General

Parametric roll resonance in longitudinal (head and following) seas is observed as a significant amplification of roll motions, which may become dangerous to the ship, its cargo and crew. This phenomenon is related to the periodic change of stability as the ship moves in longitudinal waves at a speed when the ship's wave encounter frequency is approximately twice the rolling natural frequency and the damping of the ship to dissipate the parametric roll energy is insufficient to avoid the onset of a resonant condition.

1.2 Stability in Longitudinal Waves

If a ship is located in a wave trough, the average waterplane width is significantly greater than in calm water. The flared parts of the bow and stern are more deeply immersed than in calm water and the wall-sided midship is less deep. This makes the mean, instantaneous waterplane wider than in calm water with the result that the metacentric height (GM) is increased over the calm water value. (See Section 1, Figure 1)

FIGURE 1
Profile of Waterline in Wave Trough (Solid) vs. Calm Water (Dotted)

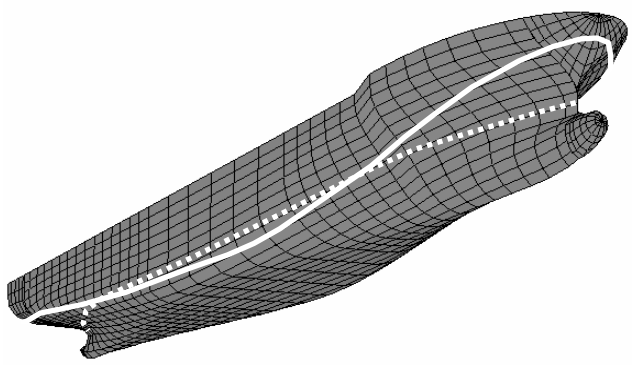

In contrast to the above, when the wave crest is located amidships, the waterplane at the immersed portions of the bow and stern are narrower than in calm water. Consequently, the average waterplane is narrower and the GM is correspondingly decreased in comparison to calm water (see Section 1, Figure 2). As a result, the roll restoring moment of the ship changes as a function of the wave's longitudinal position along the ship.

FIGURE 2
Profile of Waterline in Wave Crest (Solid) vs. Calm Water (Dotted)

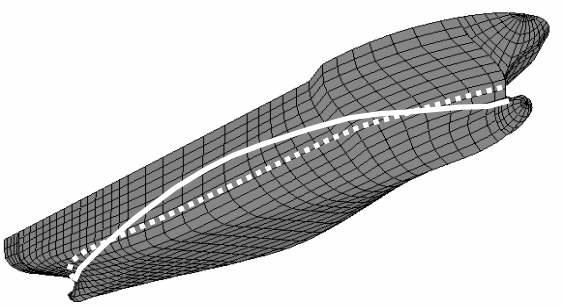

1.3 Roll Motions in Calm Water

When a ship is in calm water, any disturbance in transversal (as from a wind gust) will lead to roll motions. When the roll equilibrium is disturbed, the hydrostatic restoring moment acts to oppose the instantaneous roll angle and tends to return the ship back to the upright position. Because of inertia, the ship does not stop at the instant when the equilibrium angle is reached but continues to roll at a progressively slower velocity until a maximum roll angle is reached. At this point, the excess roll restoring moment causes the ship to begin to right itself. Once upright, inertia causes the ship to continue to roll. As before, the restoring moment works against further motion and it stops at some roll angle. The restoring moment then again pushes the ship back to the equilibrium, and again, because of inertia, the ship cannot stop at the equilibrium point and the motion cycle is repeated. The period of such roll oscillations in calm water is known as the "natural roll period" and is related to ship stability and mass distribution. The corresponding roll frequency is called the "natural frequency". A sample of such a free roll oscillation is shown in Section 1, Figure 3.

FIGURE 3
Undamped Small Roll Motions in Calm Water

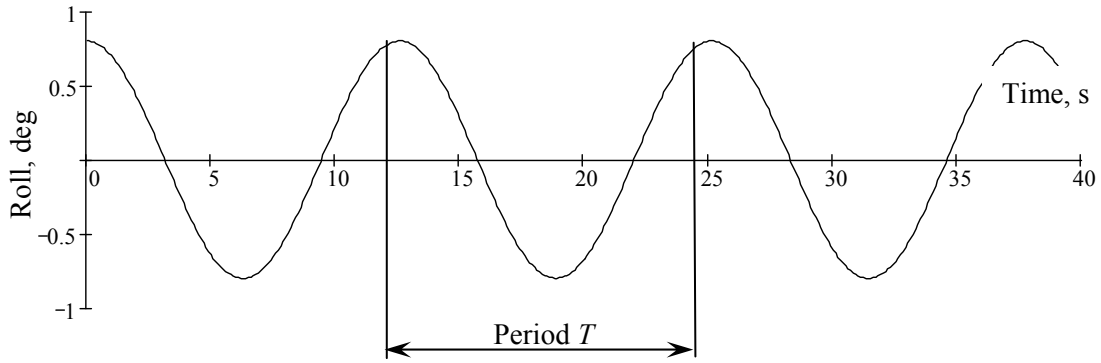

If a ship sailed on a course exactly perpendicular to the crests of head or following seas, there would be no wave–induced heeling moment. However, the ship may experience a very small roll disturbance from some external or internal cause (in reality, roll disturbances can always exist, e.g., wind). Normally, when the roll equilibrium is disturbed in the absence of a wave excitation moment, the ship rolls with its natural roll frequency and the motion time history is similar to that shown in Section 1, Figure 3

1.4 Physics of Parametric Roll Resonance

As described earlier, when a ship is sailing in longitudinal (head or following) or nearly longitudinal seas, its stability increases in the wave trough and decreases on the wave crest. If this oscillatory change in stability occurs at approximately twice the natural roll period, roll motions may increase to a significant, possibly unacceptable, angle as a result of parametric roll resonance. A typical sample time history is shown in Section 1, Figure 4.

FIGURE 4
Parametric Roll Resonance

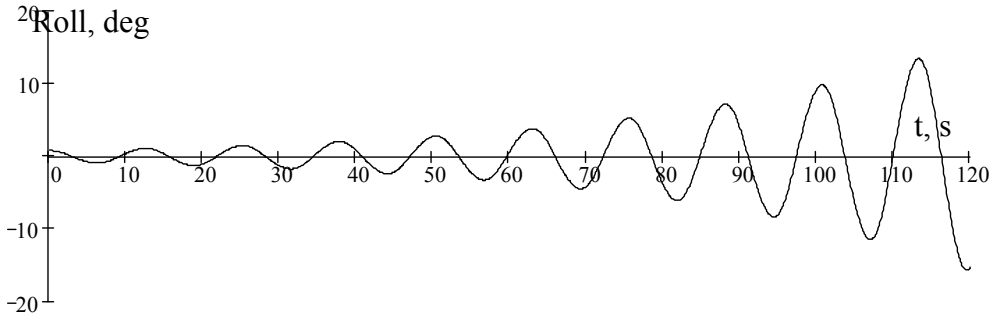

The most rapid increase of parametric roll motion could be observed when the ship experiences an external roll disturbance at the time when the wave crest is moving away from amidships, *i.e.*, the condition of improving or increasing stability, in combination with an encounter frequency approximately twice that of the natural roll frequency. In this situation, the restoring moment tends to accelerate the ship back to equilibrium with a larger-than-calm-water moment because the ship is entering the wave trough where stability is improved. As a result, at the end of the first quarter of the period *T*, the roll angle is slightly larger than it would be in calm water. See Section 1, Figure 5.

At the end of the first quarter period of roll oscillation, the ship reaches a zero-degree roll angle, which is the upright equilibrium attitude, but the roll motion does not stop there because of the roll inertia.

During the second quarter of the period, the ship encounters a wave crest and its stability is decreased. Meanwhile, the roll motion inertia makes the ship continue to roll. The restoring moment now resists further motion, but with a less-than-calm-water value since ship stability is lessened on the wave crest. As a result, the ship rolls more than it would in calm water with the same roll disturbance, consequently, after the second quarter, the increase in roll angle is even greater than after the first quarter. This is shown in Section 1, Figure 5.

In the third quarter, the ship enters the wave trough and an increased restoring moment pushes it back with an increased force. The situation is analogous to that observed during the first quarter. The observations in the fourth quarter are similar to those in the second quarter, and the roll angle continues to increase, as shown in Section 1, Figure 5.

With no further change in wave amplitude and ship speed, this combination of restoring (with a larger-than-calm-water) and resisting the roll (with less-than-calm-water) can cause the roll angle to progressively increase to a large and possibly dangerous level. This constitutes the parametric roll resonance phenomenon.

FIGURE 5
Development of Parametric Roll Resonance;
Case 1: Ship Encounters Roll Disturbance when Stability is Increasing

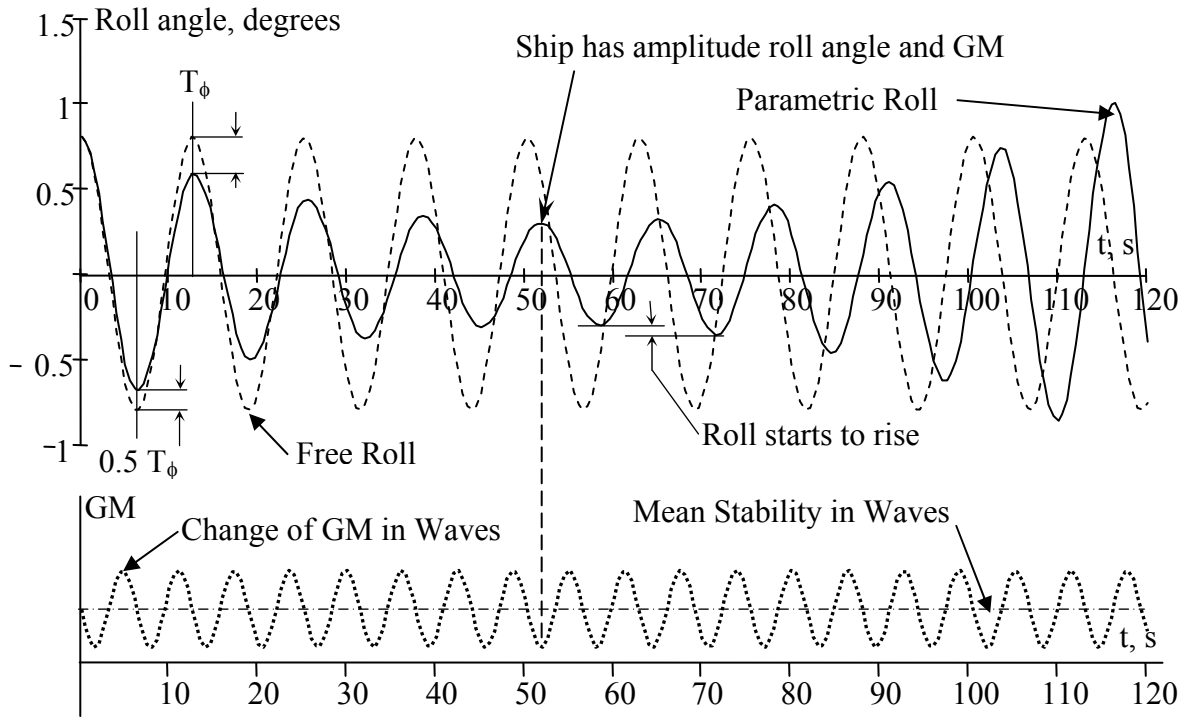

If the ship experiences the roll disturbance while approaching a wave crest, i.e., when the stability is decreasing, the evolution of parametric roll development is different.

The same factors that were increasing roll in the first case now damp the roll motion. When the ship is just disturbed, it approaches a wave crest with its stability decreased and the "push back" is made with a smaller moment than in calm water. Once the ship reaches equilibrium, its stability starts to improve and it reaches a less-than-in-calm-water angle at the end of the first period. See Section 1, Figure 6.

Such a combination of decreasing and increasing roll restoring moments is capable of significantly decreasing roll. However, this situation does not last long. The changing stability leads to a slight change in the natural period. As a result, the roll in waves lags behind in comparison with the roll in calm water. See Section 1, Figure 6.

As can be seen from Section 1, Figure 6, the shifting phase leads to a situation where the ship reaches a peak value of roll angle and as its GM is just about to start to increase. This situation is similar to the conditions considered in the previous case.

The two considered sample scenarios represent two extreme possibilities with the most and least favorable conditions for the development of parametric roll. The real situation is usually somewhere in between.

FIGURE 6
Development of Parametric Roll Resonance; Case 2: Ship Encounters Roll Disturbance when Stability is Decreasing

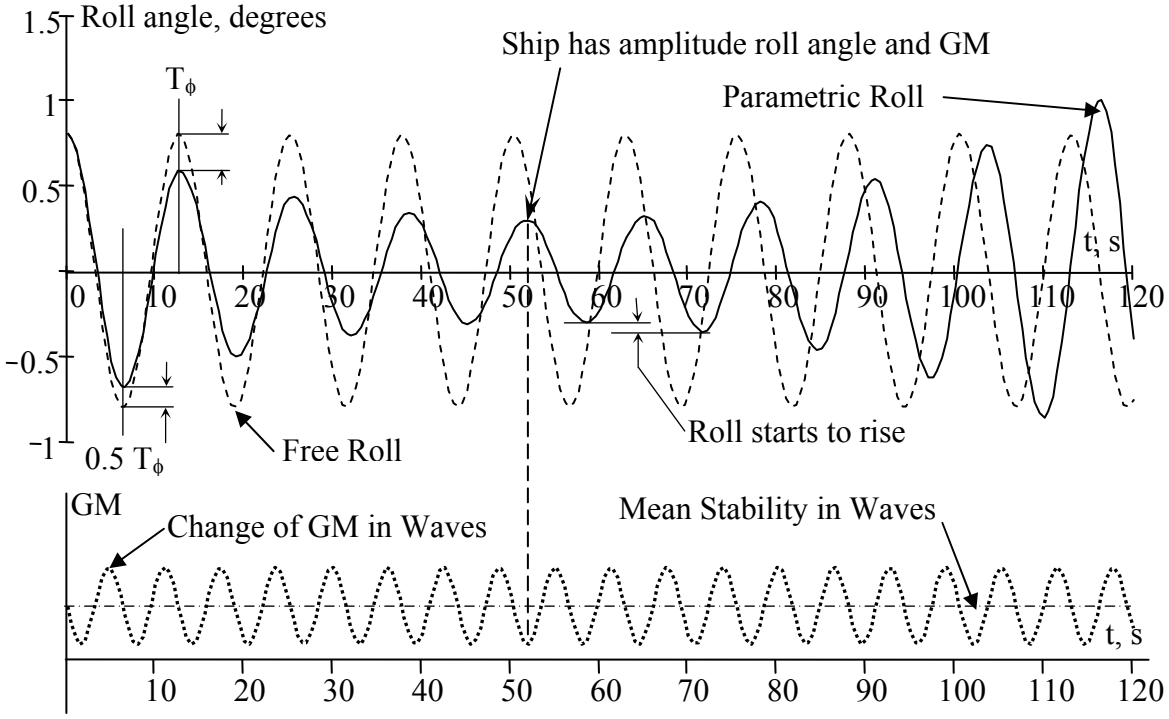

1.5 Influence of Roll Damping

When a ship rolls in calm water after being disturbed, the roll amplitudes decrease successively due to roll damping. See Section 1, Figure 7. A rolling ship generates waves and eddies, and experiences viscous drag. All of these processes contribute to roll damping.

FIGURE 7
Successively Decreasing Roll Amplitudes due to Roll Damping in Calm Water

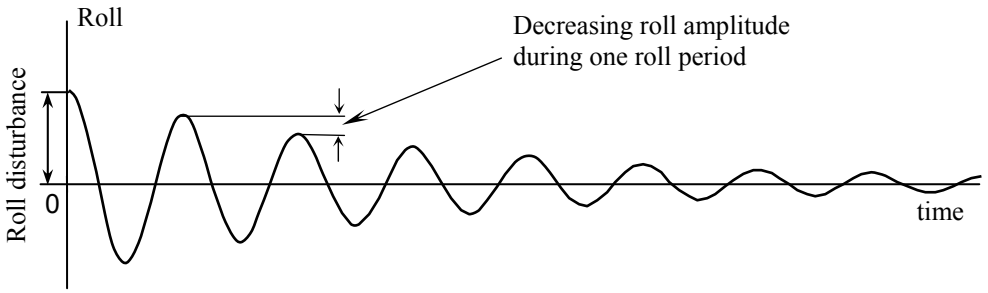

Roll damping may play a critical role in the development of parametric roll resonance. If the "loss" of energy per cycle caused by damping is more than the energy "gain" caused by the changing stability in longitudinal seas, the roll angles will not increase and the parametric resonance will not develop. Once the energy "gain" per cycle is more than the energy "loss" due to damping, the amplitude of the parametric roll starts to grow.

There is then a roll damping threshold for parametric roll resonance. If the roll damping moment is higher than the threshold, then parametric roll resonance is not possible. If the roll damping moment is below the threshold, then the parametric roll resonance can take place.

During the parametric roll resonance the combination of harder push-backs due to the increased stability on the wave trough and larger achieved roll angles due to the decreased stability on the wave crest, which occur about twice during the roll period, makes the roll angle grow significantly. The only other condition that has to be met is that the energy loss due to roll damping is not large enough to completely consume the increase of energy caused by parametric roll resonance – the roll damping is below the threshold value.

1.6 Amplitude of Parametric Roll

The shape of the GZ curve is one of the most important factors determining the amplitude of parametric roll. As discussed in 1/1.4, the development of parametric roll requires the encounter wave frequency to be approximately twice the roll natural frequency. There is a range of encounter wave frequencies around this value that is capable of causing parametric roll resonance.

It is known that the instantaneous value of GM is a function of roll angle (see Section 1, Figure 8). It is also known that the natural roll period and natural roll frequency depend on GM value. While the GZ curve usually is practically linear in the first 10-12 degrees of heel angle, the GM does not change, so both natural roll period and frequency remain constant for small values of roll angle (up to about 10-12 degrees).

Once the roll angle increases beyond the linear portion of the GZ curve, the instantaneous GM value changes as the GZ curve bends (see Section 1, Figure 8). This causes the natural roll period and natural roll frequency to change as well. Since the wave encounter frequency remains the same, the roll natural frequency may no longer be close to twice the encounter frequency. As a result, parametric resonance conditions no longer exist and roll motions no longer receive additional energy at each cycle. This causes parametric roll to stop increasing and a certain amplitude of roll is established (see Section 1, Figure 9).

FIGURE 8
Change of Instantaneous GM Value with Increasing Heel Angle

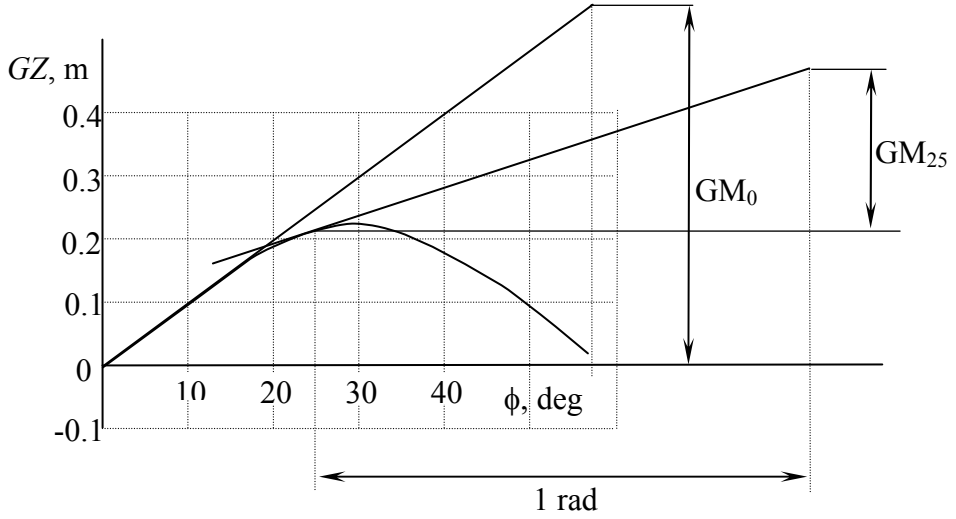

FIGURE 9
Development of Parametric Roll

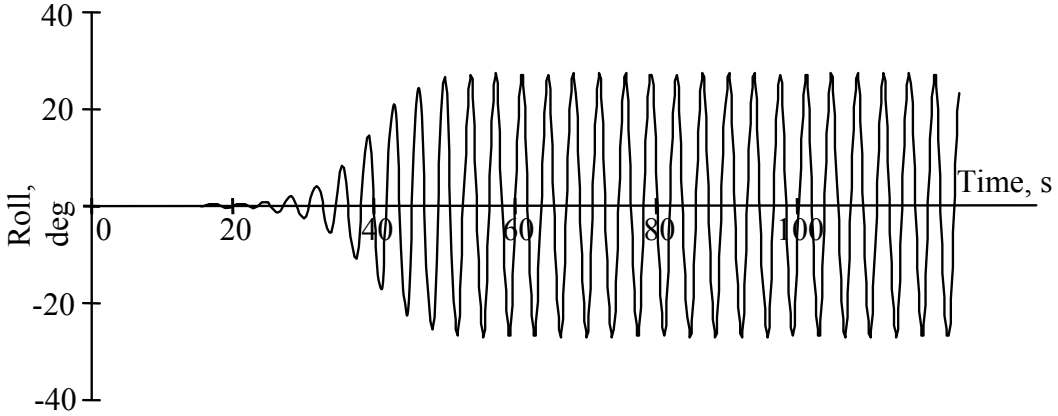

1.7 Influence of Ahead Speed and Wave Direction

Longitudinal waves (head and following) cause the most change in ship's intact stability and, therefore, create maximum parametric excitation. This Guide considers head and following seas only, as these situations potentially pose the greatest danger of development of parametric roll resonance.

A ship moving though the waves encounters them with a different frequency than a ship that is not moving. This frequency is called "frequency of encounter" or "encounter frequency". It is smaller for following seas (ship speed is subtracted from wave celerity) and larger for head seas (wave celerity is added to ship ahead speed).

Frequency of encounter is a frequency with which a ship passes through wave crests and troughs. The encounter period (wave period corresponding to the wave frequency of encounter) is the time that passes while a ship encounters two adjacent wave crests or two adjacent wave troughs. It is also a frequency of change of ship's stability.

Parametric roll resonance develops when the frequency of stability change is nearly twice that of natural roll frequency or when the frequency of encounter is nearly twice that of natural roll frequency. The value of natural roll frequency mostly depends on GM value (transversal distribution of weight also may have an influence). Therefore, whether parametric roll resonance may occur in following or head seas depends mostly on current GM value. Wave length also has an influence because it is related to the wave frequency on which the frequency of encounter is dependent.

Despite the physical background of parametric roll resonance in following and head seas being identical, the latter one may experience the influence of heave and pitch motions, which are more pronounced in head seas. At this moment, the Guide does not consider such an influence.

1.8 Definitions

Parametric roll – roll motion in the regime of *parametric resonance*

Parametric roll resonance – dynamic amplification of roll motions caused by periodic change of ship *stability in longitudinal (head or following) waves*

Stability in longitudinal waves – improving ship *stability in the wave trough* and decreasing *stability on the wave crest*, provided that the ship is moving or is located in head or following waves

Stability on the wave crest – stability of a ship measured by conventional characteristics such as metacentric height (GM) and GZ curve, with wave crest amidships. Usually, stability characteristics are decreased in comparison with calm water

Stability in the wave trough - stability of a ship measured by conventional characteristics such as metacentric height (GM) and GZ curve, with wave trough amidships. Usually, stability characteristics are increased in comparison with calm water.

Wave period – time between two consecutive wave crests or wave troughs passing the fixed reference point.

Wave frequency – frequency corresponding to *wave period*

Wave celerity – velocity of wave propagation

Period of encounter - time between two consecutive wave crests or wave troughs passing the moving reference point

Frequency of encounter – frequency corresponding to *Period of encounter*

Free roll oscillations – roll motion in calm water that take place if a ship was inclined on angle less than 10 degrees and then was set free to roll.

Natural roll period –period of *free roll oscillations* or time necessary for a ship to roll from minimum roll angle to maximum roll angle, or from maximum roll angle to minimum roll angle

Natural roll frequency – frequency corresponding to *natural roll period*

1.9 Nomenclature

All ship-related values are defined in the coordinate system shown in Section 1, Figure 10

B	molded breadth
d_m	a molded draft amidships
D_m	a molded depth amidships
$d(x_i\, x_{Cj})$	a molded draft of i-th station with j-th position of the wave crest, see Section 1, Figure 11

$y(x_i\, x_{Cj})$	offsets – half-breadth of i-th station at draft $d_{C\,i}$, see Section 1, Figure 12
$BM(x_{Cj})$	metacentric radius for calculated i-th position of the wave crest
GM	metacentric height (GM value) defined as a distance between transverse roll metacenter and center of gravity in calm water
$GM_{\min}$	minimum metacentric height (GM value) in waves
$GM_{\max}$	maximum metacentric height (GM value) in waves
GM_a	magnitude of change of metacentric height (GM value) between wave trough and wave crest and is calculated as the difference between $GM_{\min}$ and $GM_{\max}$
GM_m	mean value of metacentric height (GM value) averaged between wave trough and wave crest: $(GM_{\max} + GM_{\min})/2$
L	length of a ship measured between perpendiculars
V_s	ahead speed, knots
V_{pr}	ahead speed, corresponding to encounter frequency twice of roll natural frequency – "parametric roll speed", knots
V	ahead speed, m/s
$VCB(x_{Cj})$	vertical position of buoyancy center calculated i-th position of the wave crest
T_W	period of wave
ω_0	roll natural frequency in calm water
ω_m	roll natural frequency corresponding to mean value of metacentric height
ω_a	roll natural frequency corresponding to magnitude of change of metacentric height
ω_W	frequency of wave
λ	length of wave
μ	roll damping expressed as fraction of critical roll damping

FIGURE 10
Coordinate System for Hydrostatic Calculations

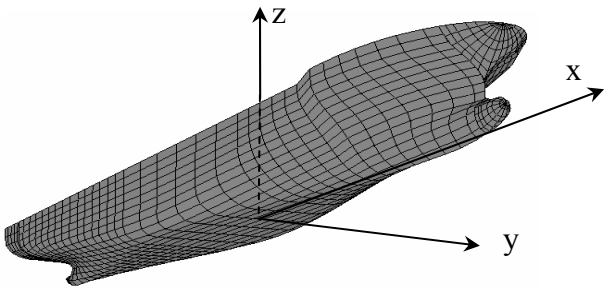

FIGURE 11
Definition of the Draft *i*-th Station with *j*-th Position of the Wave Crest

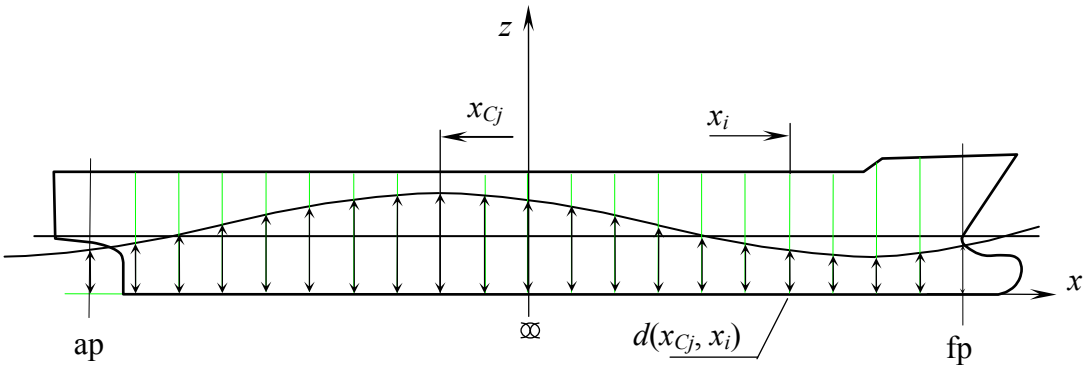

FIGURE 12
Definition of the Offsets at *i*-th Station with *j*-th Position of the Wave Crest

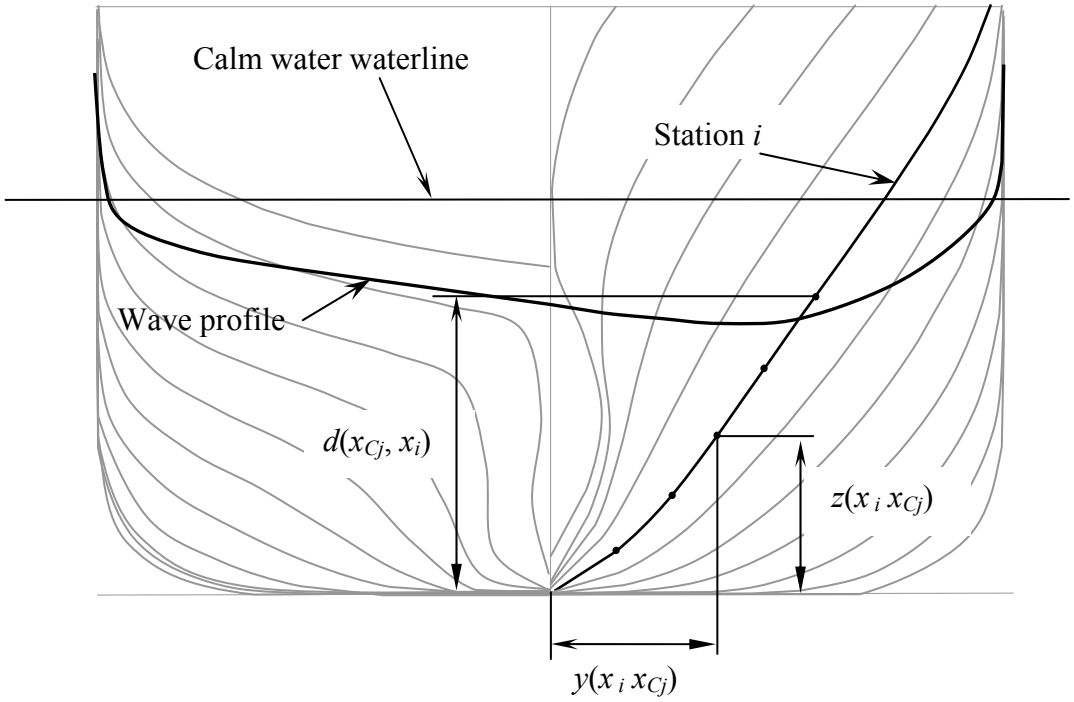

SECTION 2 Parametric Roll Criteria

1 General

Application of any criteria or performing any calculations related to parametric roll resonance requires reliable data on roll damping. At this moment, the only robust method to obtain roll damping data is a roll decay test. The roll decay test, performed by an ABS-recognized facility (normally, a towing tank – member of ITTC – International Towing Tank Conference and possessing proper certification), is required for an optional class notation (see Section 5). As an alternative, roll damping can be assumed as recommended in 2/2.4.

The general sequence of calculations and checks is described below.

The calculations and checks are done for design wave and ahead speed which will most likely lead to the development of parametric roll. These conditions are: wave length equals ship length and ahead speed results in a frequency of encounter that is about twice the roll natural frequency. If such a speed falls into the operational range of speeds, all further calculations are done for the above conditions.

If such speed does not fall into the operational range, the calculations are done for highest operational speed (design speed) and wave length equal to ship length. Additionally, the calculations are to be done for the wave length leading to encounter frequency about twice that of the roll natural frequency and the design speed. See the diagram in Section 2, Figure 1 for the choice of wave and speed conditions.

The calculations include the following steps. Stability in waves is to be computed for a number of positions of wave crest along the hull, then maximal and minimal GM values are to be evaluated. Maximal GM value is expected when the wave trough is close to amidships and the minimum GM value is expected when the wave crest is close to (but not necessarily exactly at) amidships.

The difference between maximum and minimum values defines the amplitude of parametric excitation. In order for the susceptibility criteria to be used, the parametric excitation is presented in the form of a value oscillating as sinusoidal function about the mean value, which is obtained by averaging the GM from the above-mentioned calculations. This averaged GM is used to evaluate ahead speed. The procedure is illustrated in Section 2, Figure 1.

If any of these checks indicate susceptibly, the severity of parametric roll is to be checked with a simplified numerical procedure described in Subsection 2/3. A sample of both susceptibility and severity checks can be found in Appendix 1.

Indicated severity is to be considered as a warning of a possible problem with parametric roll, which has to be addressed during further design. Sophisticated numerical simulations and model tests are to be considered. General requirements for such numerical simulations and model tests are described in Section 3. Based on the results of the numerical simulations and model tests, operational guidance is to be developed. One of the possible formats of this guidance is presented in Appendix 2.

FIGURE 1
Diagram Showing Selection of Wave Length and Ahead Speed

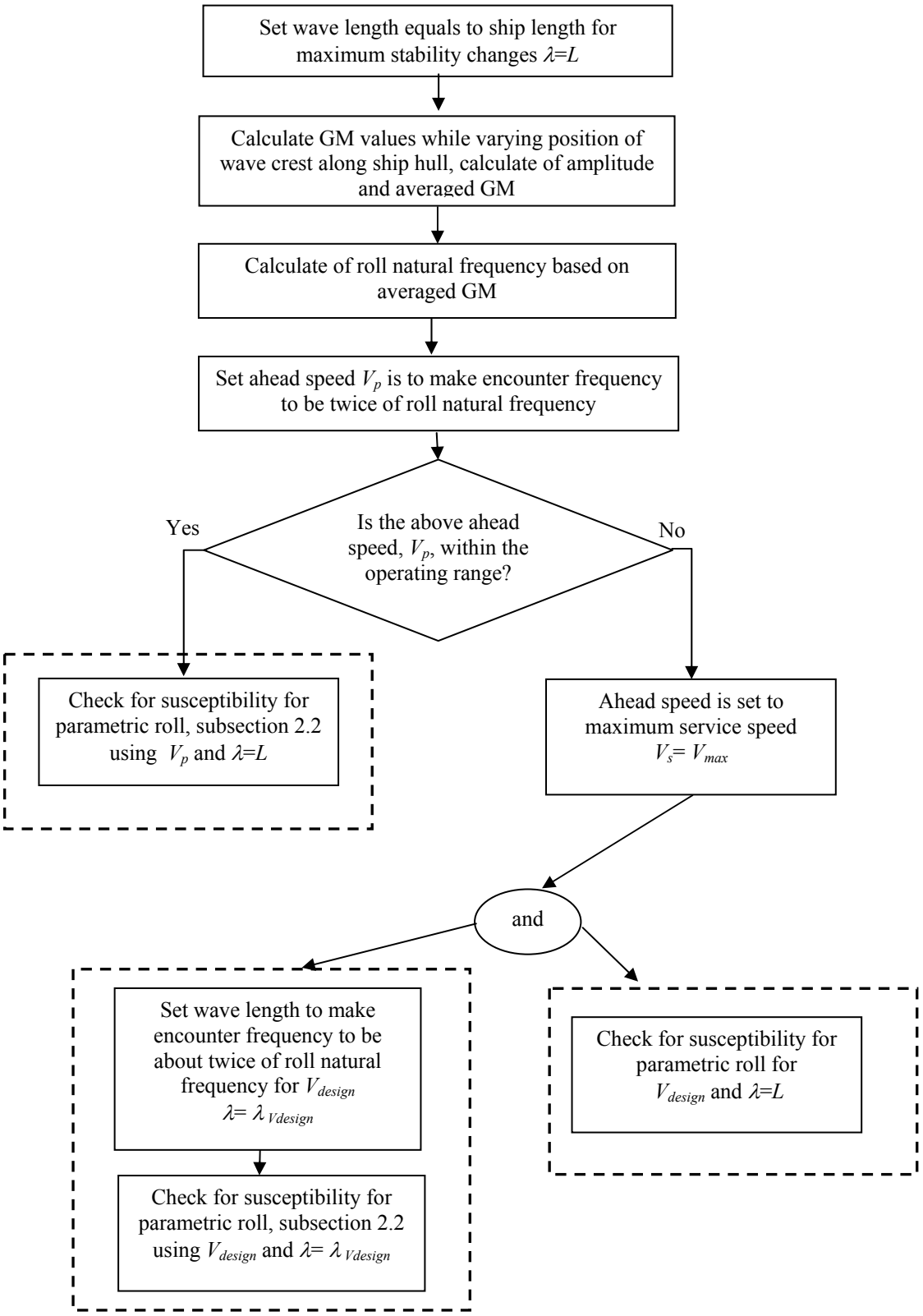

2 Susceptibility Criteria

2.1 Design Wave

Stability in longitudinal seas and parametric roll susceptibility criteria is to be calculated for the design wave. The length of the design wave, λ, is equal to the length between perpendiculars, L.

$$\lambda = L$$

The wave height is specified from Section 2, Table 1, which is based on the wave scatter table from IACS Recommendation No. 34, "Standard Wave Data" and represents waves of different lengths with the same probability of encounter.

TABLE 1
Wave Heights

Wave length λ, m	50	100	150	200	250	300	350	400	450
Wave height h_W, m	5.9	11.6	14.2	15.1	15.2	14.6	13.6	12.0	9.9

Linear interpolation may be used for intermediate wave lengths. The wave height need not exceed $2(D_m - d_m)$. Where D_m is a molded depth amidships and d_m is a molded draft amidships

Period of wave T_W corresponding to the accepted wave length should be calculated as:

$$T_W = \sqrt{\frac{2\pi\lambda}{g}} = 0.8\sqrt{\lambda} \text{ , seconds, for } L \text{ in meters}$$

Wave frequency:

$$\omega_W = \frac{2\pi}{T_W} \text{, rad/s}$$

2.2 Stability in Longitudinal Waves

Stability in longitudinal waves is to be calculated by any appropriate method. The accuracy of the method is to be demonstrated to the satisfaction of ABS.

Alternatively, it is acceptable to use the method described below (assumed coordinate system shown in Section 1, Figure 10).

Note: This method assumes that the draft of the ship in the wave, as measured relative to the mean wave surface, is the same as the still water draft. Therefore, the wave-induced pitch and heave motions are ignored.

It is recommended to use offsets presented for at least 21 stations as well as at least 21 equally spaced wave crest positions.

The draft at each station at x_i for each wave crest position x_{Cj} (see Section 1, Figure 11 for the reference) should be calculated as:

$$d(x_i, x_{Cj}) = d_m + 0.5h_w \cos\left(\frac{2\pi(x_i - x_{Cj})}{\lambda}\right)$$

The half beam $y(x_i, x_{Cj})$ at each station (see Section 1, Figure 12 for the reference) for each wave crest position should be determined by linear interpolation at station drafts $d(x_i, x_{Cj})$, calculated above.

The transverse moment of inertia of the waterline for each wave crest position is calculated as:

$$I_X(x_{Cj}) = \frac{2}{3}\int_{-0.5L}^{0,5L}[y(x, x_{Cj})]^3\,dx$$

It is recommended that the trapezoid method be used for the integration.

The submerged area at each station for each position of wave crest can be calculated as:

$$\Omega(x_i, x_{Ci}) = \int_0^{d_C(x_i, x_{Cj})} y(x_i, x_{Cj}, z)dz$$

The volumetric displacement for each wave crest position can be calculated as:

$$\nabla(x_{Cj}) = 2\int_{-0.5L}^{0.5L}\Omega(x, x_{Cj})dx$$

The vertical static moment of the submerged area at each station for each wave crest position can be calculated as:

$$M_\Omega(x_i, x_{Cj}) = \int_0^{d_C(x_i)} z \cdot y(x_i, x_{Cj}, z)dz$$

The vertical position of the center of buoyancy for each wave crest position can be calculated as:

$$VCB(x_{Cj}) = \frac{2}{\nabla}\int_{-0.5L}^{0.5L} M_\Omega(x, x_{Cj})dx$$

The metacentric radii for each position of wave crest can be calculated as:

$$BM(x_{Cj}) = \frac{I_X(x_{Cj})}{\nabla(x_{Cj})}$$

The metacentric height for each wave crest position can be calculated as:

$$GM(x_{Cj}) = BM(x_{Cj}) - KG + VCB(x_{Cj})$$

It is expected that the value of *GM* for the wave crest near amidships is smaller than the value in calm water. It is also expected that the value of *GM* for the wave trough near amidships is larger than the value in calm water (see Section 2, Figure 2). Section 2, Figure 3 shows the *GM* value as a function of the wave crest position along the hull.

Minimum and maximum values of the function $GM(x_C)$ are to be evaluated as:

$$GM_{\max} = \max[GM(x_{Cj})] \qquad GM_{\min} = \min[GM(x_{Cj})]$$

Amplitude of stability change in longitudinal seas:

$$GM_a = 0.5(GM_{\max} - GM_{\min})$$

The criteria should be evaluated for the mean values of *GM,* defined as:

$$GM_m = 0.5(GM_{\max} + GM_{\min})$$

Amplitude of stability change in longitudinal waves expressed in terms of frequency:

$$\omega_a = \frac{7.85\sqrt{GM_a}}{B}\ \text{, rad/s}$$

Mean value of stability change in longitudinal waves expressed in terms of frequency:

$$\omega_m = \frac{7.85\sqrt{GM_m}}{B} \text{ , rad/s}$$

FIGURE 2
Change of Stability in Longitudinal Wave

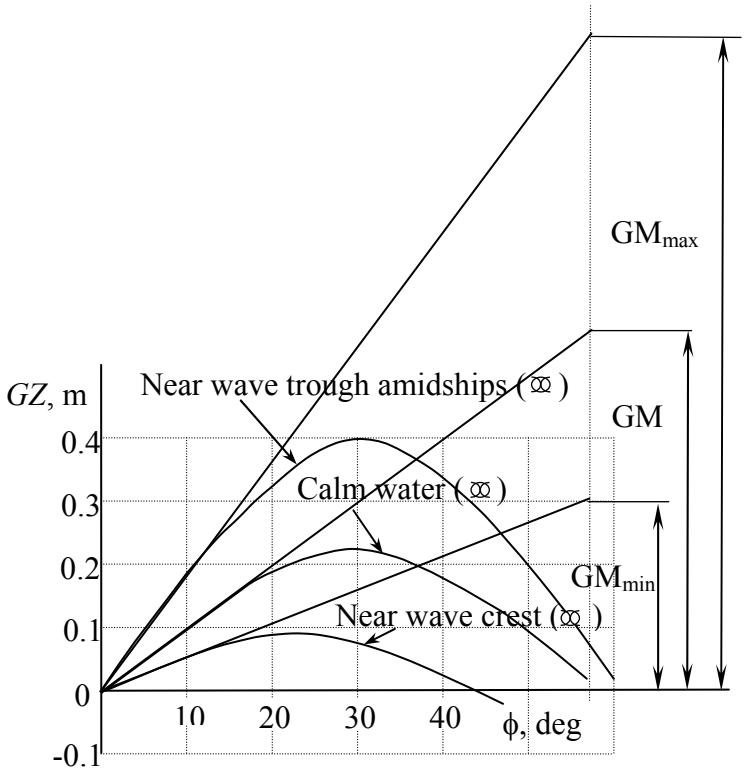

FIGURE 3
GM as a Function of Wave Crest Position

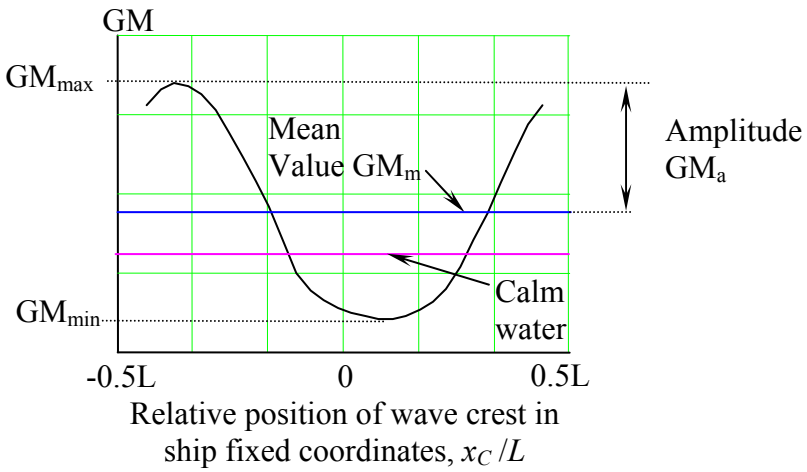

2.3 Ahead Speed

Parametric roll is most likely when the encounter frequency is approximately twice the natural roll frequency.

If the wave frequency, ω_W, is smaller than twice that of roll natural frequency in waves, $2\omega_m$, parametric roll resonance may be expected in head seas. If it is larger, the parametric roll may be expected in following seas

The speed for parametric roll is calculated:

$$V_{pr} = \frac{19.06 \cdot |2\omega_m - \omega_w|}{\omega_W^2}, \text{ kn}$$

The expression $|2\omega_m - \omega_W|$ is to be taken as absolute value.

If speed V_{pr} is not within operational range, the calculation is to be done for the achievable speed closest to that defined with the above equation. In most cases, it will be the maximum service speed, V_{sr}:

$$V_S = V_{pr} \quad \text{if } V_{pr} < V_{sr} \quad \ldots\ldots (1)$$

$$V_S = V_{sr} \quad \text{if } V_{pr} > V_{sr} \quad \ldots\ldots (2)$$

In addition to the above, if a ship is not capable of sustaining speed V_{pr} (condition 2), all of the calculations are to be repeated for the following wave frequency:

$$\omega_w = \frac{\sqrt{(96.23 + 78.48 V_S \omega_m)} - 9.807}{2V_S}, \text{ Rad/s, where } V_S = V_{sr}$$

The above wave frequency corresponds to the following wave length:

$$\lambda = \frac{61.61}{\omega_W^2}, \text{ m}$$

2.4 Application of Susceptibility Criteria

This Section describes criteria for determining whether a ship may be susceptible to parametric resonance. Technical background of these criteria can be found in ([1]).

Frequency of encounter:

Head seas: $E = \omega_E = \omega_W + 0.0524 \cdot V_S \cdot \omega_W^2$, rad/s

Following seas: $E = \omega_E = \omega_W - 0.0524 \cdot V_S \cdot \omega_W^2$, rad/s

Parameters of susceptibility criterion:

$$p = \frac{\omega_m^2 - (\mu \cdot \omega_0)^2}{\omega_E^2}$$

$$q = \frac{\omega_a^2}{\omega_E^2}$$

[1] Shin, Y., Belenky, V.L., Paulling, J.R., Weems, K.M and W.M. Lin "Criteria for Parametric Roll of Large Containerships in Head Seas", presented at SNAME Annual Meeting 2004 (available for download at http://www.eagle.org/rules/downloads.html).

Here, ω_0 is the natural roll frequency in calm water. In the absence of available data, ω_0 can be calculated as:

$$\omega_0 = \frac{7.854\sqrt{GM}}{B} \text{ , rad/s}$$

A roll decay test, performed by an ABS-recognized facility, is considered as the only reliable source of roll damping data. Alternatively, the following linear roll damping coefficient expressed as a fraction of critical damping can be assumed:

$$\mu = 0.03$$

The ship may be susceptible to parametric roll if the following inequality is satisfied:

$$0.25 - 0.5 \cdot q - 0.125 \cdot q^2 + 0.03125 \cdot q^3 - \frac{q^4}{384} \le p \le 0.25 + 0.5 \cdot q \quad \text{.....(1)}$$

If the inequality (1) is not satisfied, the ship may not be susceptible to parametric roll.

If inequality (1) is met, the damping criterion of susceptibility is to be checked:

$$\mu \frac{\omega_0}{\omega_E} < q \cdot k_1 \cdot k_2 \sqrt{1 - k_3^2} \quad \text{.....(2)}$$

Where coefficients k_1, k_2 and k_3 are to be calculated with the following formulae:

$$k_1 = 1 - 0.1875q^2$$

$$k_2 = 1.002p + 0.16q + 0.759$$

$$k_3 = \frac{q^2 - 16 + \sqrt{q^4 + 352q^2 + 1024p}}{16q}$$

If $k_3 > 1$, the damping criterion is considered as not satisfied.

If $k_3 < 1$ and inequality (2) is not satisfied, the ship's susceptibility to parametric roll is unlikely.

If both inequalities (1) and (2) are satisfied, the severity criterion in Subsection 2/3 is to be checked.

3 Severity Criterion for Parametric Roll Resonance in Head Seas

Once the susceptibility to parametric roll has been determined in Subsection 2/2, the severity of parametric roll is to be checked by means of a simplified numerical procedure.

Such a procedure involves numerical integration of the roll equation with a nonlinear restoring term taking into account the change in stability in waves. It is recommended to use actual GZ curves calculated for different wave crest positions as the wave passes along the ship (15-18 wave positions and 12-15 roll angles are recommended). As a result, the restoring term is represented as a surface in coordinates: wave position and angle of roll (see Section 2, Figure 4).

Any commercially available software capable of numerical integration of ordinary differential equations may be used. The following equation is to be solved numerically:

$$\ddot{\phi} + 2\mu\omega_0\dot{\phi} + \omega_0^2 f(\phi, t) = 0$$

The restoring term $f(\phi, t)$ should be based with two-dimensional interpolation of calculated values of the GZ curve. The following formula is recommended:

$$f(\phi,t) = \frac{sign(\phi)}{\mathrm{GM}_0} GZ(|\phi|,t)$$

Function $sign(\phi)$ is defined as –1 if the value of roll angle ϕ is negative and +1 if positive. Symbol $|\phi|$ signifies absolute value.

The following formula is to be used for the relationship between the time t and position x of the wave crest relative to amidships:

$$x = V \cdot t - L \cdot floor\left(\frac{V \cdot t}{\lambda}\right)$$

The numerical function *floor* is defined as the greatest integer number smaller than the argument $(V \cdot t/L)$. V is a speed of encounter that is to be calculated as:

$V = V_S + 0.159\omega_W\lambda$ For head seas

$V = V_S - 0.159\omega_W\lambda$ For following seas

As a result, the restoring term is a periodic odd function of two arguments, as illustrated in Section 2, Figure 5. Note that this function may have non-sinusoidal character along time axis, which is caused by the geometric difference between bow and stern hull forms.

In the absence of model test data, calculations are to be performed for the following range of roll damping coefficients:

μ = 0.03, 0.05, 0.075, 0.10

Wave conditions are to be taken as determined in 2/2.1.

The calculations should be performed for a number of ahead speeds, covering the entire range of speeds leading to parametric roll within the service range of speed. At least seven values are to be used. The following speeds must be included:

$$V_1 = \frac{19.06 \cdot |2\omega_0 - \omega_w|}{\omega_w^2}; \quad V_2 = \frac{19.06 \cdot |2\omega_m - \omega_w|}{\omega_w^2}$$

Here, ω_m is to be calculated as described in 2/2.2, and with the GM values calculated with the same software as that used for the GZ curve.

The numerical solution is to be calculated for the duration of at least 20 roll periods to achieve stabilization of the amplitude of parametric roll. An initial roll angle in the range 5 degrees is recommended to speed up the possible development of parametric roll. Several combinations of initial roll angle and angular velocity should be used since the outcome may be dependent on initial conditions.

FIGURE 4
Restoring Moment as a Function of Wave Position and Heel Angle

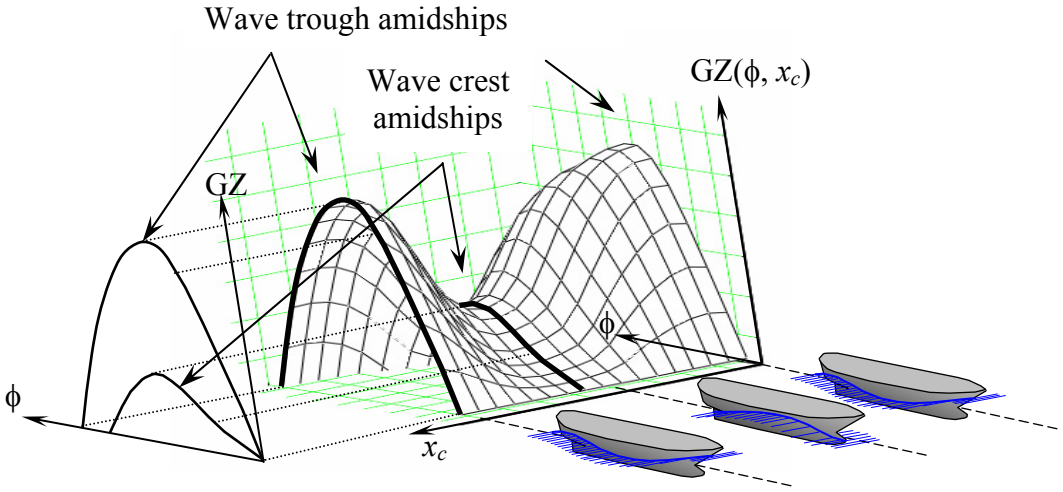

FIGURE 5
Restoring Term as a Function of Time and Heel Angle

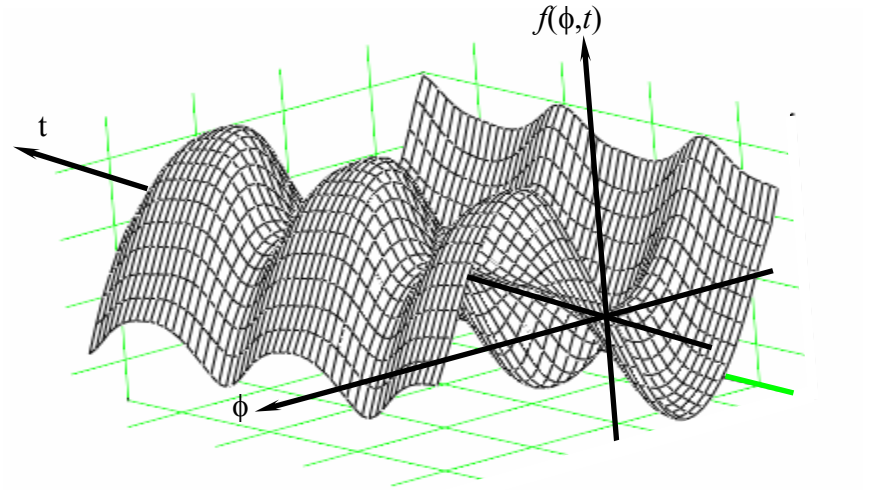

If all resulting time histories indicate decaying roll motions, the ship may not be susceptible to parametric roll.

If a time history contains oscillations reaching a steady state with their amplitude at stabilization less then 15 degrees, parametric roll at these particular conditions may be considered as posing no danger.

If any of the time histories show that the amplitude at stabilization exceeds 15 degrees or if unlimited increase of roll angle is observed, the parametric roll should be regarded as “severe”, in which case, a model test and numerical simulations are required to actually evaluate the magnitude of the problem.

This Page Intentionally Left Blank

SECTION 3 Numerical Simulations *(1 June 2008)*

If the susceptibility to parametric roll has been determined in Section 2, numerical simulations are required.

As guidance, it is recommended that a numerical simulation system based on potential hydrodynamic formulation be used, capable of calculation of *hydrostatic* and *Froude-Krylov* forces and moments over an instantaneous submerged body. *Hydrodynamic* forces and moments can be calculated over the average waterline. The simulation system should be capable of taking into account viscous and eddy-making components of roll damping as external terms from the roll decay test. Sample of such simulation technology is described in ([2]).

Numerical simulations are to be performed for representative loading conditions included in Stability and Trim Booklet and should include at least three degrees of freedom: heave, roll and pitch.

Numerical simulations are to be carried out for irregular seas for the entire range of service speeds; recommended increment is 5 knots.

Numerical simulations in irregular seas are to be performed for long-crested waves. Bretschnieder or JONSWAP spectrum is to be used. Simulations are to be carried out for the range of wave directions from 0 degrees (following seas) to 180 degrees (head seas) in 15 degrees increments and for a number of sea states starting from sea state 6 and above.

Simulation for each loading condition, sea state, speed and wave direction should be repeated at least 5 times with the same spectrum but with the different set of initial phase angles. The duration of each calculation is to be at least 12 minutes, so the total time for each condition is to be at least 3600 seconds.

The set of frequencies chosen for representation of irregular waves has to cover the entire spectral range where values of spectral density exceed 1% of maximum spectral density.

The set of frequencies must provide statistically representative restoration of time series of wave elevations. If frequencies are evenly distributed, the frequency step is to be calculated as:

$$\Delta\omega = \frac{2\pi}{T_R}, \text{ rad/s}$$

where T_R, is duration of calculation in seconds.

The maximum roll angle is to be determined from all these runs.

The plan for numerical simulations, including loading conditions as well as wave characteristics, should be approved by ABS prior to conduction the simulations.

[2] Y.S.Shin, V.L.Belenky , Y.M.Lin, K.Weems, A.Engle "Nonlinear Time Domain Simulation Technology for Seakeeping and Wave Load Analysis for Modern Ship Design", SNAME Annual Meeting 2003, San-Francisco.

This Page Intentionally Left Blank

SECTION 4

Mitigation of Parametric Roll Resonance

1 Operational Guidance *(1 June 2008)*

If a ship is found to be susceptible to parametric roll resonance, the Master should be supplied with the operational guidance indicating dangerous regimes for the representative loading conditions, and sea state where parametric roll may represent danger.

Such operational guidance may be developed for use by the Master in the form of hard copy or electronic information.

The operational guidance may be presented in the form of 'polar diagram' (wave heading angle vs. speed for each sea state and loading condition), based on numerical simulations in irregular seas as described in Section 3. The diagram shows area of different colors corresponding to maximum observed roll angles exceeding 22.5 degrees. Scale of angles and colors is to chosen as appropriate for practical use. Example of color scale along with the sample polar diagram is shown in Section 4, Figure 1. Each polar diagram must be clearly marked with loading conditions and significant wave height and characteristic wave period.

Operational Guidance is subject to ABS approval as a condition of optional class notation.

As the operational guidance may contain significant amount of information, an electronic or computerized version of the guidance is acceptable in addition to the written guidance to enhance availability of information and reduce the chance of human error.

2 Anti-Rolling Devices

If a ship is found to be susceptible to parametric roll resonance, the installation of an anti-rolling device is to be considered.

The anti-rolling device may be specifically designed to mitigate parametric roll resonance. Alternatively, if an installation of a general-purpose anti-rolling device is planned, consideration may be given to the possibility of using this device to mitigate parametric roll resonance.

If a ship is to be equipped with anti-rolling device, additional numerical simulations are required: all the calculations described in the Section 3 are to be repeated with functioning anti-rolling device.

Anti-rolling device is considered to be effective if it is capable of illuminating dangerous rolling motion to not exceed the level defined in Subsection 4/1 with less than 10% change of speed and/or 10 degrees change of course.

If the ship is to be equipped with an anti-rolling device, the operational guidance should be provided for all conditions with the anti-rolling device turned on and off.

FIGURE 1
Example of Polar Diagram and Color Scale *(1 June 2008)*

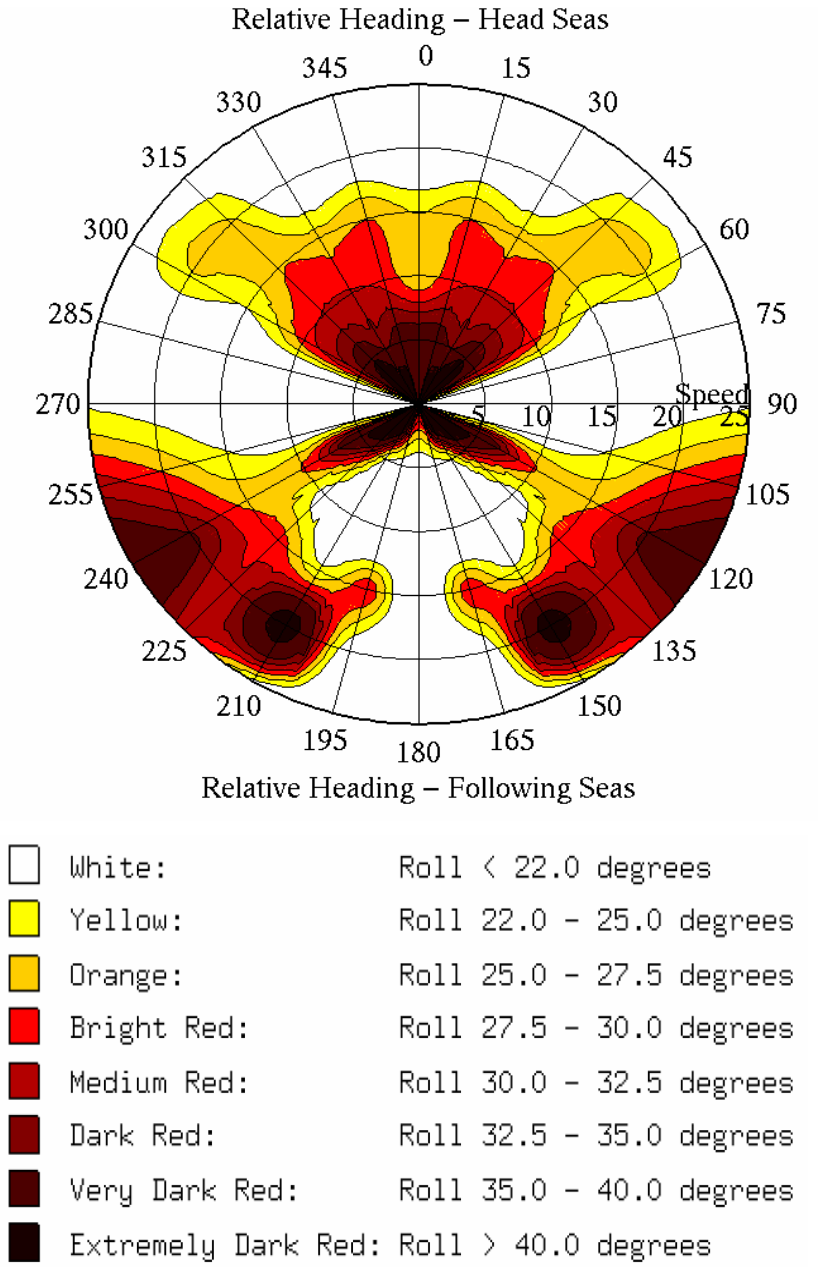

SECTION 5 Optional Class Notation

In recognition of demonstrated safety performance in relation to parametric roll resonance, ABS may assign optional class notations. A summary of requirements and a brief description is given in Section 5, Table 1.

TABLE 1
Optional Class Notations

Notation	*Description*	*Requirements*
PARR-N	No susceptibility to parametric roll	Susceptibility criteria shows no susceptibility for parametric roll (Section 2)
PARR-C1	Parametric roll under control	1. Roll decay test 2. Susceptibility and severity check (Section 2) 3. Numerical simulations performed. (Section 3) 4. Operational guidance is developed (Section 4)
PARR-C2	Parametric roll under control	1. Roll decay test 2. Susceptibility and severity check (Section 2) 3. Numerical simulations performed. (Section 3) 4. Operational guidance is developed (Section 4) 5. Anti-rolling device designed specifically to eliminate or mitigate parametric roll with proof of efficiency, or general-purpose anti-rolling devices are to be proven to be effective against parametric roll. and are to be developed and verified with model tests (Section 4)

To assign these optional notation ABS will perform limited check of the calculations described in Sections 2, 3 and 4 of this Guide. In order to perform these checks, the following information is to be submitted along with the results of calculations:

1. Lines
2. ASCII file with offset data in the following format:

   Number of stations

   For each station: Distance from FP, Number of points per station

   For each point: Z-coordinate and Y coordinate for the station as defined in Section 1, Figure 12.
3. Loading conditions: displacement, draft molded at forward and aft perpendicular, three coordinates of the center of gravity, and three radii of gyration.
4. Results of roll decay test.

This Page Intentionally Left Blank

APPENDIX 1 Sample Calculations

Lines of a container carrier used in this sample are given in Appendix 1, Figure 1. Details of the ship are shown in Appendix 1, Table 1. Wave conditions were chosen as described in Section 2 and shown in Appendix 1, Table 2. GM values are calculated for different positions of wave crest, and the results are shown in Appendix 1, Table 3 and Appendix 1, Figure 2. Ahead speed has been calculated as described in Section 2, and results are given in Appendix 1, Table 4.

FIGURE 1
Lines of Sample Container Carrier

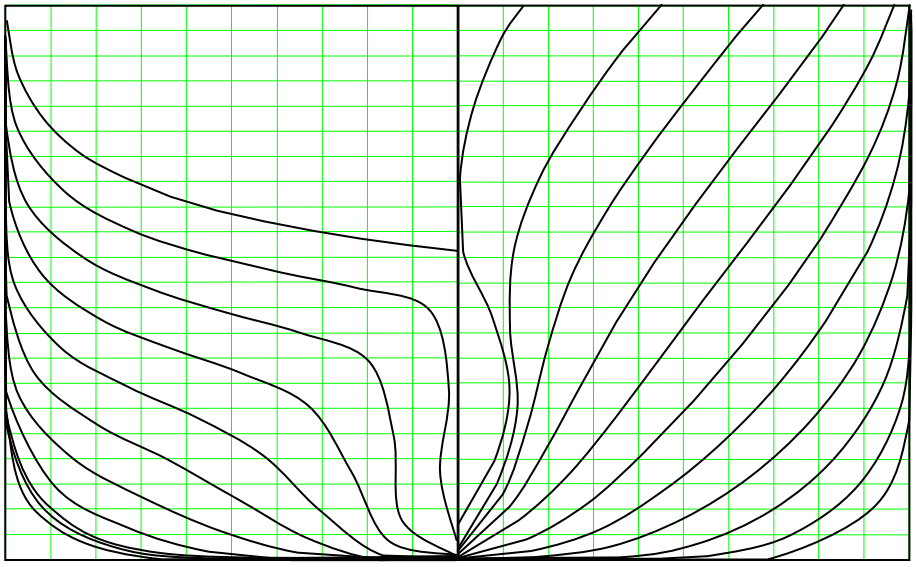

TABLE 1
Particulars of a Sample Container Carrier

Length B.P., m	262
Breadth Molded, m	40.0
Depth, m	27.4
Design draft, m	12.36
KG, m	17.55

TABLE 2
Conditions for Sample Calculations

Wave length (equals to ship length), m	262
Wave height (linear interpolation from Table 1), m	15.06
Wave period, s	12.95
Circular wave frequency ω_W, rad/s	0.485

TABLE 3
Calculation of GM Value for Different Positions of Wave Crest along Ship Hull (Simplified Method – 2/2.2)

Position of wave crest *m*	*Volumetric Displacement* m^3	*BM* *m*	*KB* *m*	*GM* *m*
-131.00	61154	16.32	8.43	7.21
-119.09	59838	17.46	8.29	8.20
-107.18	59597	17.58	8.26	8.30
-95.27	60518	16.28	8.37	7.10
-83.36	62768	13.93	8.57	4.95
-71.45	66619	11.86	8.81	3.13
-59.55	71592	10.87	9.01	2.33
-47.64	76336	10.21	9.13	1.79
-35.73	80459	9.66	9.20	1.32
-23.82	83761	9.34	9.24	1.03
-11.91	86137	9.12	9.26	0.83
0.00	87545	9.02	9.27	0.74
11.91	87977	9.09	9.29	0.83
23.82	87429	9.18	9.30	0.94
35.73	86053	9.45	9.31	1.22
47.64	83858	9.80	9.32	1.57
59.55	81115	10.31	9.31	2.07
71.45	77748	10.93	9.28	2.66
83.36	74074	11.75	9.20	3.41
95.27	70242	12.61	9.07	4.14
107.18	66580	13.67	8.88	5.00
119.09	63453	14.94	8.64	6.03
131.00	61154	16.32	8.43	7.21

FIGURE 2
Calculation of GM Value for Different Positions of Wave Crest along Ship Hull (Simplified Method – 2/2.2)

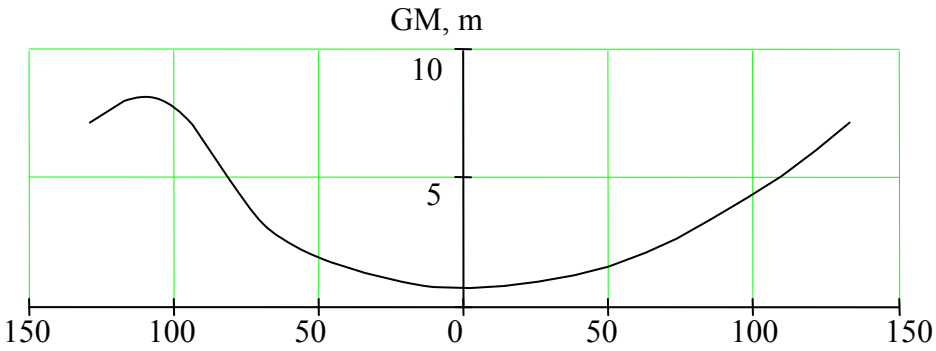

TABLE 4
Sample Results for Susceptibility Criteria

Value	*Symbol*	*Formula or data source*	*Result*
Minimum GM value, m	$GM_{\min}$	Table A-3	0.74
Maximum GM value, m	$GM_{\max}$	Table A-3	8.30
Amplitude of parametric excitation, m	GM_a	$GM_a = 0.5(GM_{\max} - GM_{\min})$	3.77
Mean value of *GM*	GM_m	$GM_m = 0.5(GM_{\max} + GM_{\min})$	4.52
Amplitude of stability change in longitudinal waves expressed in terms of frequency, Rad/s	ω_a	$\omega_a = \left(7.854\sqrt{GM_a}\right)/B$	0.382
Mean value of stability change in longitudinal waves expressed in terms of frequency, Rad/s	ω_m	$\omega_m = \left(7.854\sqrt{GM_m}\right)/B$	0.417
Forward speed most likely for development of parametric roll, kn	V_{pr}	$V_{pr} = \dfrac{19.06\lvert 2\omega_m - \omega_w\rvert}{\omega_w^2}$	28.4
Frequency of encounter, Rad/sec.	ω_E	$\omega_E = \omega_W + 0.0524 \cdot V_S \cdot \omega_W^2$	0.835
GM value in calm water m	*GM*		2.48
Natural roll frequency in calm water, Rad/s	ω_0	$\omega_0 = \left(7.854\sqrt{GM}\right)/B$	0.309
Roll damping coefficient expressed as a fraction of critical damping	μ		0.1
Parameter of susceptibility criterion:	p	$p = \left(\omega_m^2 - (\mu \cdot \omega_0)^2\right)/\omega_E^2$	0.249
Parameter of susceptibility criterion:	q	$q = \omega_a^2 / \omega_E^2$	0.209

TABLE 4 (continued)
Sample Results for Susceptibility Criteria

Value	*Symbol*	*Formula or data source*	*Result*
Left boundary of inequality (1)	$0.25 - 0.5 \cdot q - 0.125 \cdot q^2 + 0.03125 \cdot q^3$		0.140
Right boundary of inequality (1)	$0.25 + 0.5 \cdot q$		0.354
Susceptibility inequality (1) outcome	**Positive**		
Coefficient k_1 of damping criterion	$k_1 = 1 - 0.1875 \cdot q^2$		0.992
Coefficient k_2 of damping criterion	$k_2 = 1.002p + 0.16q + 0.759$		1.042
Coefficient k_3 of damping criterion	$k_3 = \dfrac{q^2 - 16 + \sqrt{q^4 + 352q^2 + 1024p}}{16q}$		0.142
Boundary of damping criterion inequality (2) – damping threshold value	$q \cdot k_1 \cdot k_2 \sqrt{1 - k_3^2}$		0.205
Effective damping	$\mu \cdot \omega_0 / \omega_E$		0.037
Susceptibility inequality (2) outcome	**Positive**		

As the susceptibility criteria check was positive, the severity check is to be applied. GZ curves were calculated using the special software that includes the capability of computing stability in longitudinal waves. The program requires ship offset and wave characteristics (wave length, wave height and position of the wave crest) as an input and integrates hydrostatic pressure around the hull up to the actual wave waterline. The procedure first places the ship on the wave at the longitudinal position of wave crest specified in the input. The pitch-heave attitude of the ship is then obtained using an assumption of pitch-heave static equilibrium. This is seen to be equivalent to the traditional longitudinal bending moment computed by poising the ship in static equilibrium on a wave. Righting arms are then computed for a series of heel angles while preserving equilibrium of weight-buoyancy and trim moments at each heel angle. The results are shown in Appendix 1, Table 5 and Appendix 1, Figure 3. The difference between these results and GM values shown in Appendix 1, Table 3 is due to assumptions employed in the simplified method in 2/2.2. Calculation of the forward speed and other auxiliary values is given in Appendix 1, Table 6.

FIGURE 3
GZ Curves for Different Positions of Wave Crest

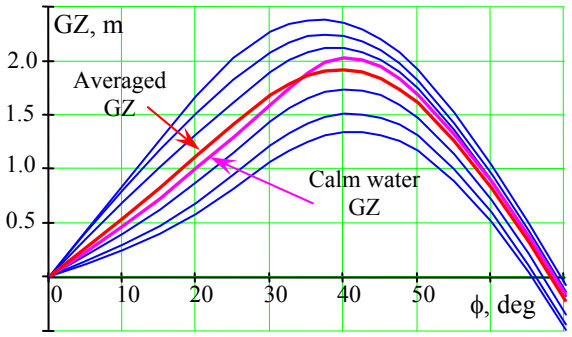

TABLE 5
GZ Curves for Different Positions of Wave Crest

	Distance from FWD Perpendicular to Wave Crest, m							
Heel Angle	*0*	*16.4*	*32.8*	*49.1*	*65.5*	*81.9*	*98.3*	*115*
0	0	0	0	0	0	0	0	0
5	0.589	0.618	0.576	0.511	0.432	0.317	0.181	0.112
10	1.17	1.2	1.12	0.987	0.826	0.619	0.376	0.235
15	1.71	1.73	1.62	1.42	1.18	0.903	0.589	0.379
20	2.16	2.15	2.02	1.79	1.51	1.18	0.827	0.565
25	2.43	2.4	2.28	2.09	1.81	1.46	1.08	0.752
30	2.53	2.5	2.4	2.26	2.03	1.69	1.29	0.902
35	2.49	2.46	2.38	2.28	2.12	1.82	1.42	1
40	2.35	2.32	2.26	2.2	2.08	1.83	1.46	1.05
45	2.13	2.1	2.06	2.02	1.91	1.74	1.38	1
50	1.83	1.8	1.77	1.74	1.67	1.5	1.21	0.839
55	1.46	1.43	1.41	1.37	1.31	1.14	0.894	0.586
60	1.02	0.987	0.953	0.915	0.847	0.697	0.493	0.201
65	0.509	0.472	0.431	0.398	0.324	0.194-	0.00565	-0.257
70	-0.0465	-0.0878	-0.13	-0.165	-0.239	-0.354	-0.56	-0.785
GM, m	6.77	7.17	6.67	5.95	5.03	3.67	2.05	1.25

TABLE 5 (continued)
GZ Curves for Different Positions of Wave Crest

	Distance from FWD Perpendicular to Wave Crest, m							
Heel Angle	*131*	*147*	*164*	*180*	*197*	*213*	*229*	*246*
0	0	0	0	0	0	0	0	0
5	0.091	0.0769	0.069	0.0846	0.127	0.222	0.354	0.491
10	0.194	0.166	0.154	0.18	0.27	0.456	0.721	0.989
15	0.324	0.283	0.262	0.296	0.442	0.72	1.11	1.49
20	0.485	0.433	0.405	0.444	0.65	1.03	1.53	1.97
25	0.621	0.568	0.556	0.638	0.903	1.39	1.94	2.31
30	0.719	0.656	0.669	0.816	1.15	1.72	2.21	2.46
35	0.771	0.703	0.743	0.944	1.38	1.91	2.3	2.46
40	0.765	0.702	0.766	1.01	1.5	1.96	2.24	2.34
45	0.699	0.629	0.711	1.03	1.51	1.88	2.07	2.13
50	0.539	0.472	0.58	0.928	1.36	1.67	1.81	1.84
55	0.305	0.248	0.361	0.706	1.09	1.34	1.46	1.48
60	-0.0229	-0.0761	0.0738	0.392	0.706	0.911	1.01	1.03
65	-0.445	-0.462	-0.282	-0.0103	0.252	0.419	0.498	0.523
70	-0.931	-0.918	-0.714	-0.48	-0.257	-0.119	-0.0559	-0.0329
GM, m	1.02	0.86	0.754	0.951	1.42	2.52	4.03	5.61

TABLE 6
Sample Results for Forward Speed Calculations

Value	*Symbol*	*Formula or data source*	*Result*
Minimum GM value, m	$GM_{\min}$	Appendix 1,Table 5	0.754
Maximum GM value, m	$GM_{\max}$	Appendix 1,Table 5	7.17
Mean value of *GM*	GM_m	$GM_m = 0.5(GM_{\max} + GM_{\min})$	3.676
Mean value of stability change in longitudinal waves expressed in terms of frequency, Rad/s	ω_m	$\omega_m = \left(7.854\sqrt{GM_m}\right)/B$	0.376
Natural roll frequency in calm water, Rad/s	ω_0	$\omega_0 = \left(7.854\sqrt{GM}\right)/B$	0.315
Forward speed 1, kn	V_1	$V_1 = \dfrac{5.040\lvert 2\omega_m - \omega_w\rvert}{\omega_w^2}$	11.82
Forward speed 2, kn	V_2	$V_2 = \dfrac{5.040\lvert 2\omega_0 - \omega_w\rvert}{\omega_w^2}$	21.73

GZ curves in Appendix 1, Table 4 and Appendix 1, Figure 3 are presented in the form of the surface in coordinates: wave position and angle of roll are shown in Section 2, Figure 5.

Application of the formulae for restoring term $f(\phi, t)$ from Subsection 2/2 makes it a periodical function of time when waves pass the ship. See Section 2, Figure 5.

Most software for the solution of ordinary differential equations is meant to work with systems of 1st order ordinary differential equations. The roll equation in Subsection 2/2 is a second order ordinary differential equation. In order to be solved numerically, this equation is presented as a system of two first order differential equations. This can be done considering roll velocity as the second variable:

$$\begin{cases} \dot{\vartheta} + 2\delta\vartheta + f(\phi, t) = 0 \\ \dot{\phi} - \vartheta = 0 \end{cases}$$

Most of the commercially available software requires that the above system of differential equations be presented in matrix form:

$$\dot{Y} = D(Y, t)$$

Where $\dot{Y}$ is a vector (array) of derivatives of state variables

$$\dot{Y} = \begin{pmatrix} \dot{Y}_1 \\ \dot{Y}_2 \end{pmatrix} = \begin{pmatrix} \dot{\vartheta} \\ \dot{\phi} \end{pmatrix}$$

The first component (element) of this vector (array) is roll acceleration and the second is roll velocity.

Y is another vector (array) containing state variables – roll velocity and roll angle:

$$Y = \begin{pmatrix} Y_1 \\ Y_2 \end{pmatrix} = \begin{pmatrix} \vartheta \\ \phi \end{pmatrix}$$

$D(Y, t)$ is a vector valued function whose definition is based on the system of ordinary differential equations of the first order:

$$D(Y,t) = \begin{pmatrix} -2\delta Y_1 - f(Y_2, t) \\ Y_1 \end{pmatrix}$$

Most of the commercially available software requires the user to put initial conditions for roll velocity and roll angle into the vector (array) Y and use it as input. Recommended values for initial condition are:

$$Y = \begin{pmatrix} Y_1 \\ Y_2 \end{pmatrix} \qquad \begin{pmatrix} rad/s \\ rad \end{pmatrix}$$

The rest of the input data preparation includes the choice of a time step and a range of calculation. The following values for the above figures are recommended:

Time step: Range:

$$\Delta t = \frac{0.314}{\omega_m} \qquad T_R = \frac{125.2}{\omega_m}$$

Parameters for these calculations are placed in Appendix 1, Table 7. Results of integration are shown in Appendix 1, Figure 4 (one case). Amplitudes of parametric roll are placed for all cases in Appendix 1, Table 8.

TABLE 7
Sample Input Data for Integration of Roll Equation

Value	*Symbol*	*Formula or data source*	*Result*
GM value in calm water m	*GM*		2.58
Natural roll frequency in calm water, Rad/s	ω_0	$\omega_0 = \left(7.854\sqrt{GM}\right)/B$	0.315
Roll damping coefficient	δ	$\delta = 0.05 \cdot \omega_0$	0.0158
Time step s	Δt	$\Delta t = 0.314/\omega_m$	0.829
Time range, s	T_R	$T_R = 152.2/\omega_m$	332
Initial roll angle, degree	ϕ_0		5
Initial roll velocity, degree/s	$\dot{\phi}_0$		0

FIGURE 4
Solution of the Roll Equation for V_1 and μ = 0.1

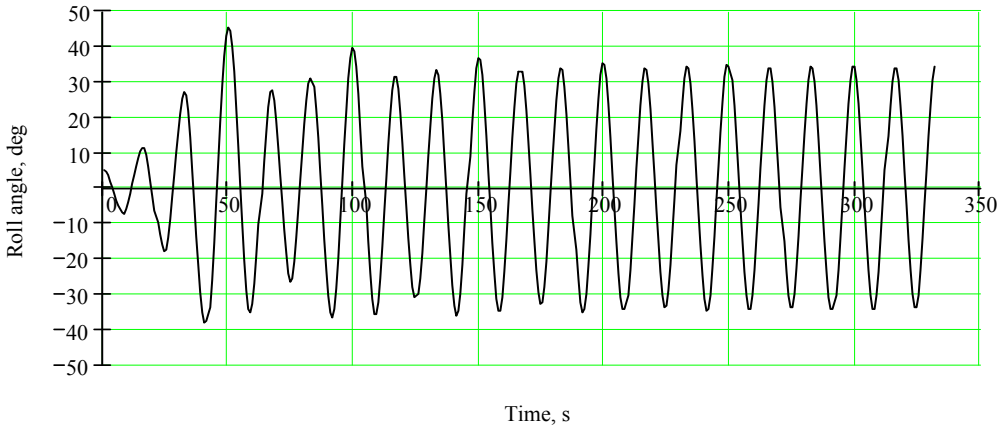

TABLE 8
Amplitude of Parametric Roll in Degrees

V, kn	μ			
	0.03	0.05	0.075	0.1
5	None	None	None	None
6	6.4	1.7	1.2	None
8	19.4	18.5	17.2	15.6
9	Unlimited	23.4	21.7	19.9
V_2 = 11.82	Unlimited	Unlimited	Unlimited	47.3
17	Unlimited	Unlimited	41.5	41.0
19	Unlimited	39.6	39.0	38.5
V_1 = 21.73	36.0	35.5	35.3	34.0
25	31.0	30.7	30.2	29.6
28	25.6	25.3	24.7	23.8

In some cases, amplitude could not be defined from the numerical integration of the rolling equation because unlimited rise of roll angle was observed. These cases are marked as “unlimited”.

As can be seen from both Appendix 1, Table 8 and Appendix 1, Figure 4, roll amplitudes were above 15 degrees in many cases, so the parametric roll should be characterized as “Severe”.

APPENDIX 2 Sample Polar Diagrams[3]

Appendix 2, Figure 1 shows a sample operational polar diagram produced with sophisticated numerical simulation (see the reference in the footnote), where roll motions exceed 20 degrees for a containership in long-crested sea state 8 conditions with a modal period of 16.4 seconds and a significant wave height of 11.49 meters. More samples of polar diagrams are shown in Appendix 2, Figures 2-7, calculated for different seas states and loading conditions.

FIGURE 1
Sample Polar Diagram

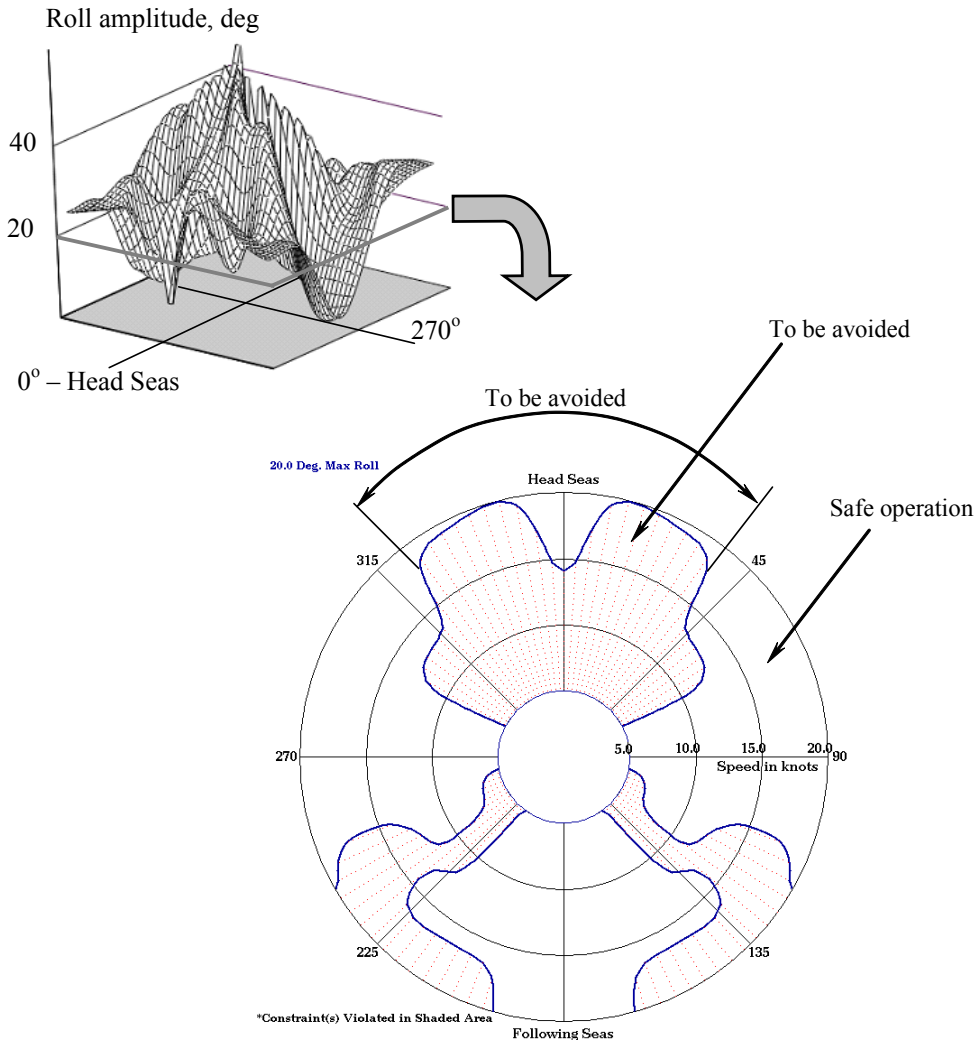

Note: This diagram is given for visual illustration only. It does not necessarily meet all of the requirements of Sections 3 and 4.

[3] Shin, Y., Belenky, V.L., Paulling, J.R., Weems, K.M and W.M. Lin "Criteria for Parametric Roll of Large Containerships in Head Seas", to be presented at SNAME Annual Meeting 2004.

The diagram is created from a series of numerical simulations from 5 through 20 knots in 5-knot increments at 15 degree heading increments. All speed/heading combinations inside of the shaded region exceed a 20-degree maximum roll angle during each 750-second simulation. The regions of higher speed and following seas correspond to a resonant roll condition where the encounter frequency is near the roll natural frequency, while the head sea regions are strictly parametric roll- induced motions. The maximum roll angle for this series of simulations is 48 degrees in the head sea 10-knot case. While no simulations were performed for speeds lower than 5 knots, it should be noted that parametric roll is still possible at lower speeds. This type of diagram can be very useful in helping the shipmaster avoid the occurrence of parametric roll while the ship is operating in severe sea conditions.

FIGURE 2
Sample Polar Diagram – Full Load, Sea State 9

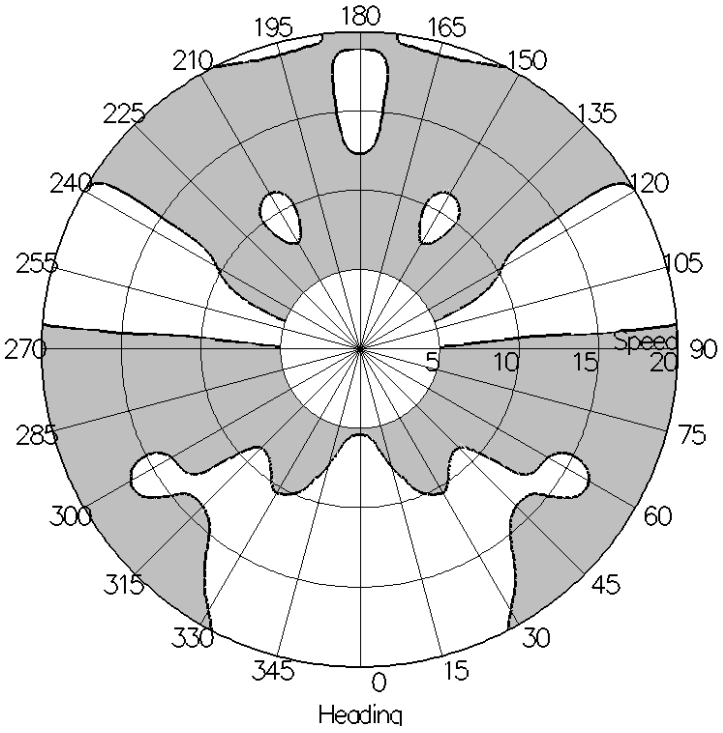

FIGURE 3
Sample Polar Diagram – Full Load, Sea State 8

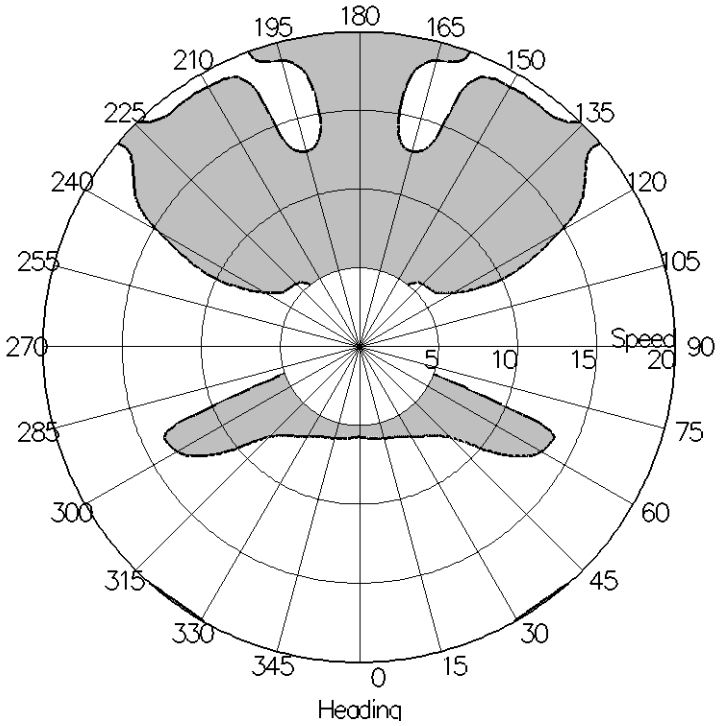

FIGURE 4
Sample Polar Diagram – Full Load, Sea State 7

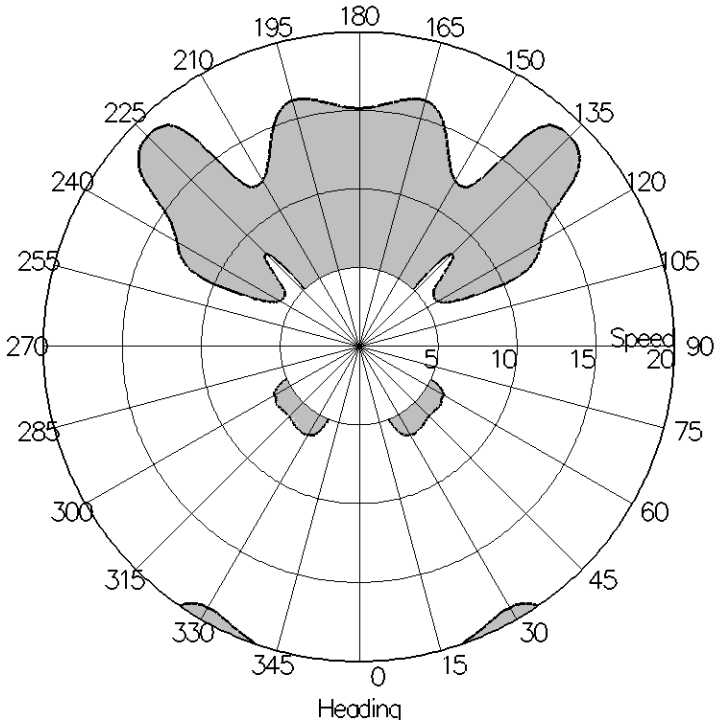

FIGURE 5
Sample Polar Diagram – Partial Load, Sea State 9

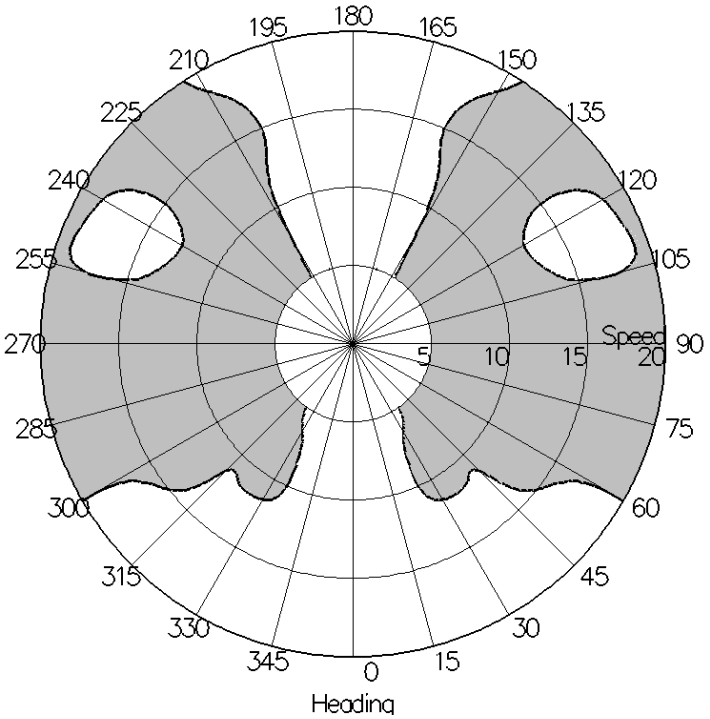

FIGURE 6
Sample Polar Diagram – Partial Load, Sea State 8

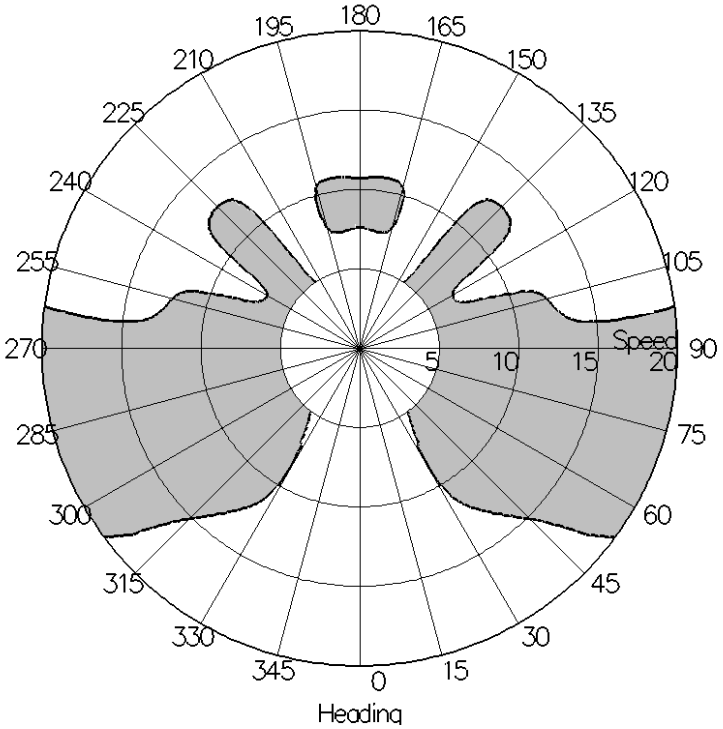

FIGURE 7
Sample Polar Diagram – Partial Load, Sea State 7

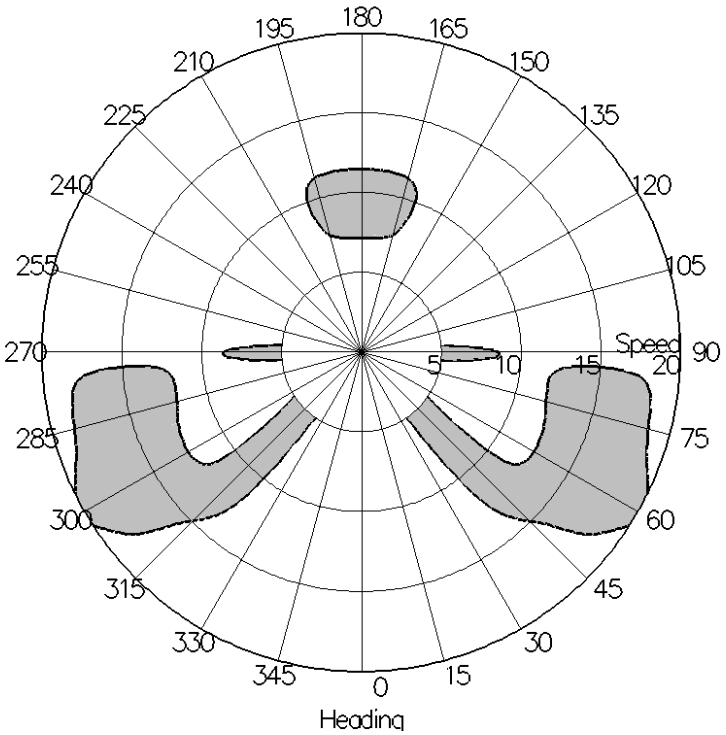

This Page Intentionally Left Blank

APPENDIX 3 Criteria for Parametric Roll of Large Containerships in Longitudinal Seas

Note: This Appendix is reprinted from a paper presented at the SNAME Annual Meeting in Washington, DC, on September 30, 2004.

Y.S. Shin, Associate Member, American Bureau of Shipping, **V.L. Belenky**, Member, American Bureau of Shipping, **J.R. Paulling,** Life Fellow, University of California at Berkeley (Ret.), **K.M. Weems**, Member, Science Applications International Corporation, **W.M. Lin**, Member, Science Applications International Corporation

ABSTRACT

This paper discusses the technical background of the American Bureau of Shipping (ABS) "Guide for the Assessment of Parametric Roll Resonance in the Design of Container Carriers." The paper, which follows the structure of the proposed Guide, begins with an explanation of the physics of the parametric roll resonance phenomenon in longitudinal (head and following) waves. This explanation does not use any mathematical models and was designed to be accessible to engineers with a variety of backgrounds. The paper has two main foci: first, the establishment of Susceptibility Criteria that can be used to determine if there is danger of parametric roll and, second, a description of methods for calculating amplitude of parametric roll in longitudinal waves that serves as a Severity Criterion. Verification of the both criteria has been done using the Large Amplitude Motions Program (LAMP), one of the most sophisticated general seakeeping simulation codes available. The paper describes the verifications that were performed, which showed that the criteria provided a very reasonable means of predicting the likelihood of occurrence of the phenomenon.

The paper also discusses probabilistic aspects of numerical simulation of parametric roll in irregular waves, and examines methods of probabilistic treatments of parametric roll.

INTRODUCTION

The phenomenon of parametrically excited roll motion has been known to naval architects for almost a half of a century [Paulling and Rosenberg, 1959, Paulling 1961]. It is caused by periodic changes of transverse stability in waves, characterized by a decrease of stability when the ship is in the wave crest and an increase in the wave trough.

The problem of parametric roll returned to prominence recently as a result of significant cargo loss and damage sustained by a Post-Panamax container carrier on a voyage from Taiwan to Seattle, Washington [France, *et al.,* 2003]. A detailed investigation followed, showing that a large roll motion with up to 35 degrees amplitude accompanied by significant pitch and yaw motion resulted from the periodic change of transverse stability in head seas. The large change of stability in head seas was found to be a direct result of the hull form. Substantial bow flare and stern overhang, now typical of large container carriers, cause a dramatic difference in waterline form – and therefore in transverse stability – between the crest and trough of a large wave.

Despite the fact that the physical nature of parametric roll has been known for many years, several new elements are present in this case. In the past, the concern had been mostly for smaller ships in following seas. Now, the concern is for the vulnerability of large container carriers in head seas. The problem is particularly important given the long-standing heavy-weather maritime practice of sailing into head seas at reduced speed. It turns out that this is not necessarily the best practice for large container carriers.

PHYSICS OF PARAMETRIC ROLL

The material included in this section is primarily intended to explain the physical nature of parametric roll without using a mathematical model. This information is also included in the proposed Guide.

Stability in Longitudinal Waves

If a typical containership is located on a wave trough, the average waterplane width is significantly greater than in calm water. Full-formed parts of the bow and stern are more deeply immersed than in calm water and the wall-sided midship is less deep. This makes the mean, instantaneous waterplane wider with the result that the *GM* is increased over the calm water value (see Figure 1).

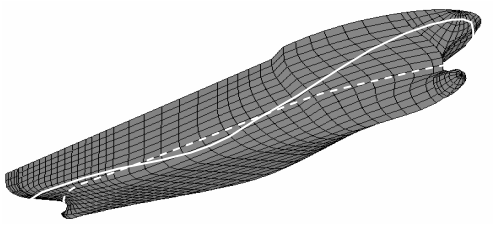

Figure 1. Form of waterline in wave trough vs. in calm water

In contrast, when the ship is located with the wave crest amidships, the immersed portion the bow and stern sections are narrower than in calm water. Consequently, the mean waterplane is narrower and the *GM* is correspondingly decreased in comparison to calm water as shown in Figure 2. As a result, the roll restoring moment of the ship will change as a function of the ship's longitudinal position relative to the waves. The waterlines in both waves and calm water are shown in Figure 3.

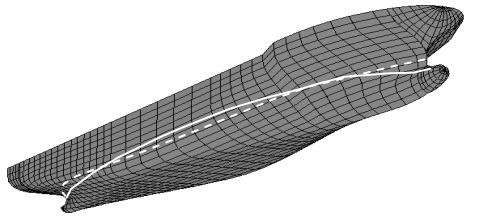

Figure 2. Form of waterline in wave crest vs. in calm water

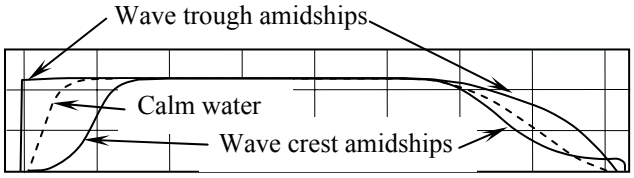

Figure 3. Form of waterline in wave crest and wave trough vs. in calm water

Roll Motions in Calm Water

When a ship is in calm water, an impulsive disturbance in roll or roll velocity (such as that caused by a wind gust) can set up an oscillatory roll motion. The period of such roll oscillations in calm water depends on the ship's stability or restoring moment properties and the mass properties, and is known as the "natural roll period." The corresponding frequency is called the "natural roll frequency". A sample of such a free roll oscillation is shown in Figure 4.

If a ship sails in head or following seas, i.e., waves in which the crests are exactly perpendicular to the ship's centerline, there will be no wave-induced heeling moment. In reality, however, there will be small external disturbances such as might be caused by wind gusts. When the roll equilibrium is disturbed in the absence of a wave excitation moment, the ship rolls with its natural roll frequency and the initial behavior is similar to that shown in Figure 4.

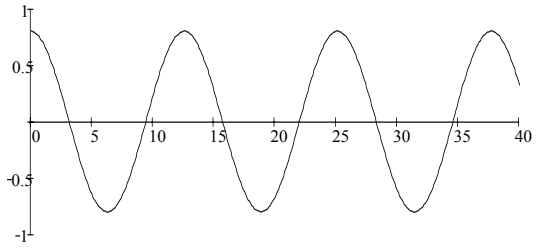

Figure 4. Sample of free roll motions

Physics of Parametric Resonance

When a ship is sailing in head seas, its stability increases when the wave trough is near amidships and decreases on the wave crest. If this stability variation occurs twice during one natural roll period, the rolling motions may build up to quite large angles as a result of parametric resonance. A typical sample record is shown in Figure 5

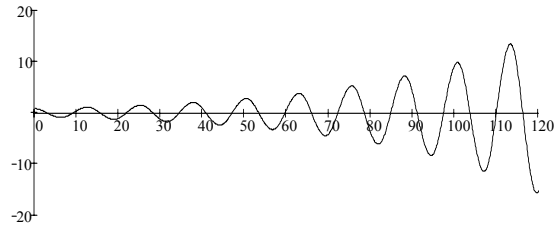

Figure 5. Sample of parametric roll (parametric resonance)

The most rapid increase of parametric roll can be observed when two conditions pertain: (1) the ship encounters the waves at a frequency near twice the natural frequency of roll, and (2) the roll disturbance occurs in the time interval between the wave crest and trough amidships position, or, as noted, when the stability is increasing. In this situation, the restoring moment, tending to return the ship to its equilibrium position, is greater than the calm water moment. As a result, after the first quarter period, the roll angle will be slightly larger than it would have been in calm water (Figure 6).

At the end of the first quarter of the period, the ship rolls back to the initial, zero degree attitude and continues to roll to the other side because of its inertia. During the second quarter of the period, the ship encounters a wave crest and the restoring moment now becomes less that the still water value. As a result, the ship rolls to a larger angle than it normally would in calm water with the same roll disturbance, and after the second quarter, the roll angle is increased to a larger value than that at the end of the first quarter. This is shown in Figure 6.

In the third quarter, the ship enters the wave trough and a restoring moment greater than the still water value now opposes the motion. The situation is analogous to that observed during the first quarter, and the observations in the fourth quarter are similar to those in the second quarter as well. The roll angle continues to increase as shown in Figure 6.

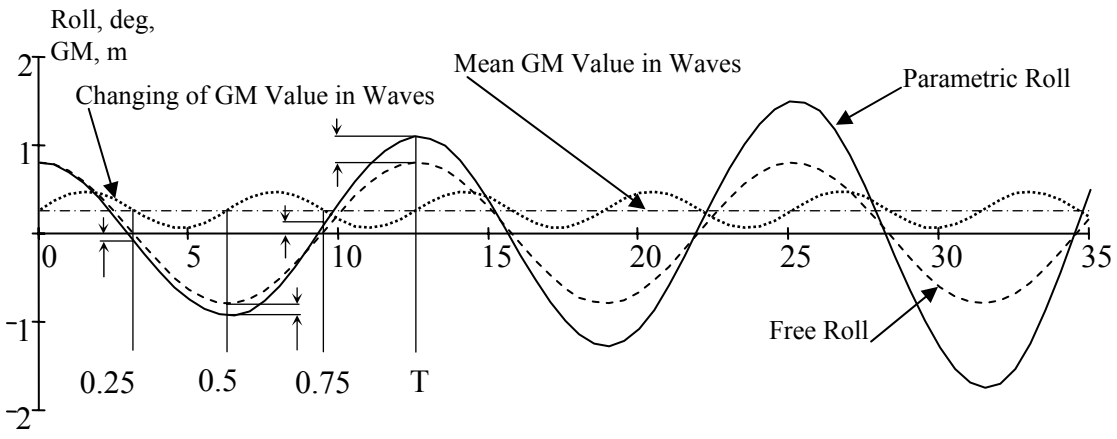

Figure 6. Development of parametric roll

Finally, the combination of restoring with a greater-than-calm-water moment and resisting the roll with less-than-calm-water moment causes the roll angle to continue to increase unless other factors come into play. This then qualitatively describes the parametric roll resonance phenomenon.

Influence of Roll Damping

When a ship rolls in calm water after being disturbed, the roll amplitudes decrease over successive periods due to roll damping (see Figure 7). A rolling ship generates waves and eddies, and experiences viscous drag. All of these processes contribute to roll damping

Roll damping plays an important role in the development of parametric roll resonance. If the "loss" of amplitude per period caused by damping is more than the "gain" caused by the changing stability in longitudinal seas, the roll angles will not increase and parametric resonance will not develop. If the "gain" per period is more than the "loss", parametric roll will grow in amplitude.

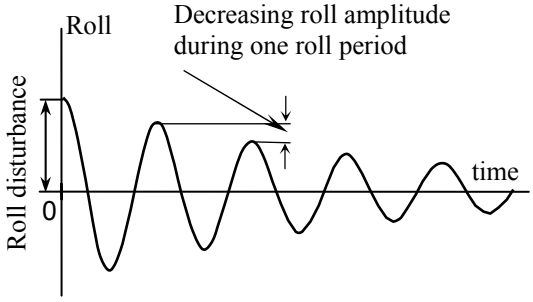

Figure 7. Successively decreasing roll amplitudes due to roll damping in calm water

This implies that there is a damping threshold for parametric resonance. If the damping is higher than the threshold, then no parametric roll is possible. If the damping is below the threshold, then parametric roll can exist.

Influence of Forward Speed and Wave Direction

Longitudinal waves (head and following) cause the most change in stability and, therefore, create maximum parametric excitation. Parametric roll resonance develops when the frequency of stability change is nearly twice that of natural roll frequency or when the frequency of encounter is nearly twice that of natural roll frequency. The value of natural roll frequency mostly depends on GM value (transversal distribution of weight also may have an influence). Therefore, whether parametric roll resonance may occur in following or head seas depends mostly on current GM value. Wave length also has an influence because it is related to the wave frequency on which the frequency of encounter is dependent. While the physical basis of parametric roll resonance in following and head seas is essentially identical, head seas parametric roll is more likely coupled with, or at least influenced by, the heave and pitch motion of the ship, as these motions are typically more pronounced in head seas.

Summary

In the preceding sections it is shown that a ship sailing in longitudinal seas experiences a time-varying transverse stability characterized by increased stability when the ship has a wave trough amidships and decreased stability in the wave crest. If such a ship experiences a small arbitrary roll disturbance, then that disturbance can grow provided that the stability fluctuations occur at a frequency approximately twice the natural frequency of roll and provided that the roll damping is less than some threshold value. This rolling motion, under certain circumstances, can grow to quite large amplitudes and is referred to as "autoparametrically excited roll" or simply "parametric roll".

STABILITY IN LONGITUDINAL SEAS

From the discussion above, it is clear that a key element in a ship's susceptibility to parametric roll is the change of stability in longitudinal seas. This section describes a relatively simple procedure for evaluating this change.

Sample Ship Data

A Post-Panamax C11-class containership was chosen as a sample in this study and is the same as that described in [France, *et al.,* 2003]. The body plan is shown in Figure 8; its principal characteristics are given in Table 1.

Table 1. Principal Dimensions of Post-Panamax C11 class container carrier

Length B.P., m	262
Breadth Molded, m	40.0
Depth, m	27.4
Design draft, m	12.36

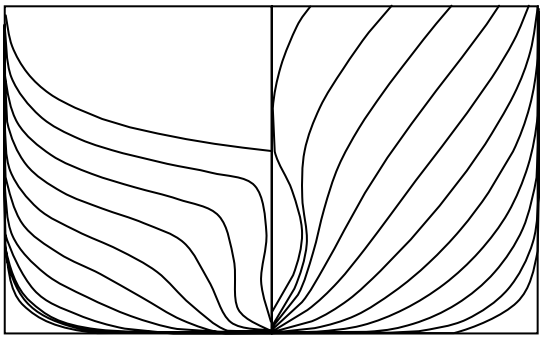

Figure 8. Lines of Post-Panamax C11 class container carrier

Spreadsheet Calculation Technique for Wave Influence on *GM*

A spreadsheet computation has been devised that provides the essential features of the varying stability as the ship moves through longitudinal waves. This simplified computation neglects the pitch-heave motions of the ship but includes the effects of wave geometry.

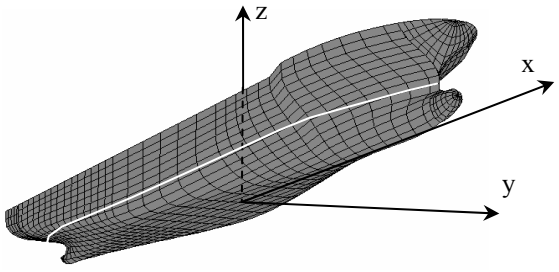

Figure 9. Coordinate system for hydrostatic calculations

The assumed coordinate system is shown in Figure 9. For a given wave length L and a height h_w, the draft at each station when the wave crest is located at x_{Cj} (amidships) can be calculated as:

$$d_C(x_i, x_{Cj}) = d_m - 0.5h_w \cos\left(\frac{2\pi(x_i - x_{Cj})}{\lambda}\right) \quad (1)$$

The half beam y_C at each station for the wave crest position at x_{Cj} is determined by interpolation of the offsets at the station's draft, $d(x_i\, x_{Cj})$, calculated by (1).

The transverse moment of inertia of the waterline for each position of the wave crest is calculated as:

$$I_X(x_{Cj}) = \frac{2}{3}\int_{-0.5L}^{0,5L} [y(x, x_{Cj})]^3\, dx \quad (2)$$

The trapezoid method may be used for the integration.

The submerged areas at each station for each wave crest position are correspondingly calculated as:

$$\Omega(x_i, x_{Ci}) = \int_0^{d_C(x_i, x_{Cj})} y(x_i, x_{Cj}, z)dz \quad (3)$$

The displacement volume for each position of the wave crest is calculated as:

$$\nabla(x_{Cj}) = 2\int_{-0.5L}^{0.5L} \Omega_C(x, x_{Cj})dx \quad (4)$$

The vertical static moment of submerged area at each station for each wave crest positions is calculated as:

$$M_\Omega(x_i, x_{Cj}) = \int_0^{d_C(x_i)} z \cdot y(x_i, x_{Cj}, z)dz \quad (5)$$

The vertical position of the center of buoyancy can be calculated as:

$$VCB(x_{Cj}) = \frac{2}{\nabla}\int_{-0.5L}^{0.5L} M_\Omega(x, x_{Cj})dx \quad (6)$$

Metacentric radii for wave crest and trough conditions can now be calculated as:

$$BM(x_{Cj}) = \frac{I_X(x_{Cj})}{\nabla(x_{Cj})} \quad (7)$$

Finally, the metacentric heights for each position of wave crest then expressed in the form:

$$GM(x_{Cj}) = BM(x_{Cj}) - KG + VCB(x_{Cj}) \quad (8)$$

Results for the Sample Ship

Intermediate and final results of the stability calculation in longitudinal wave characteristics, which are given in Table 2, are summarized in Table 3.

Table 2. Wave Characteristics

Wave length (equals to ship length), m	262
Wave height (1/20 L)	13.1
Wave period, s	12.95
Circular wave frequency rad/s	0.485

As can be seen from Table 3, there is a noticeable difference in displacement in wave crest and wave trough. The simple spreadsheet computation described above does not provide a search for equilibrium in waves. Such a procedure would call for an iterative computation that is best performed in a specialized hydrostatics code.

The program EUREKA includes the capability of computing stability in longitudinal waves. A description of the method is available in [Paulling 1961]. The program requires ship offset and wave characteristics (wave length, wave height and position of the wave crest) as an input and integrates hydrostatic pressure around the hull up to the actual wave waterline. There is an option to take into account the "Smith effect" or dynamic pressure gradient in the wave associated with the wave motion.

Table 3. Stability changes in waves calculated with simplified (spreadsheet) method

Value	**Calm water**	**Min *GM***	**Max *GM***
Volumetric displacement, m^3	70,270	85030	60,581
Weight displacement in salt water, m. ton	72,030	87,160	62,950
VCB, m	7.24	8.93	7.84
BM, m	12.78	9.38	17.29
KG, m	17.55	17.55	17.55
GM, m	2.47	0.77	7.59

The procedure first places the ship on the wave at the longitudinal position of wave crest specified in the input. The pitch-heave attitude of the ship is then obtained using an assumption of pitch-heave static equilibrium. This is seen to be equivalent to the traditional longitudinal bending moment computed by poising the ship in static equilibrium on a wave. Righting arms are then computed for a series of heel angles while preserving equilibrium of weight-buoyancy and trim moments at each heel angle.

This assumption of static equilibrium is considered suitable for representing the ship moving in following seas where the period of encounter is sufficiently low as to excite little dynamic response in pitch and heave. In order to test the resulting error if this assumption is used for head seas, some computations have been performed in which the dynamic pitch-heave attitude of the ship has been obtained by means of a linear ship motions code.

Figure 10 contains righting arms computed for the C11 containership in L/20 head and following seas using each of these assumptions. The solid and fine dashed curves contain results obtained using the static pitch-heave assumption. The other two curves were computed using pitch-heave positions from a linear strip theory computation. Results are shown for the wave crest and wave trough at amidships and it is seen that there is a small difference between the two assumptions. The *GZ* by the dynamic attitude computation displays somewhat less variation about the mean value than *GZ* obtained using the dynamic attitude of the ship. Table 4 summarizes these results as calculated by EUREKA.

The approximate calculations and EUREKA software yield a slight difference in calm water *GM*. This difference is primarily due to the fact that EUREKA generates closures for bow and stern, while the described spreadsheet calculations use the waterplane limited by the perpendiculars.

Table 4. Stability changes in waves calculated with EUREKA

Value	Calm water	Wave Crest	Wave trough
Weight Displacement in salt water, m. ton	72,370	72,370	72,370
KG, m	17.55	17.55	17.55
GM, m	2.58	1.05	6.34

More significantly, EUREKA gives smaller differences for *GM* values for the ship on the wave crest and wave trough. This means that the parametric excitation would be larger, according to the approximate calculation, which makes them more conservative.

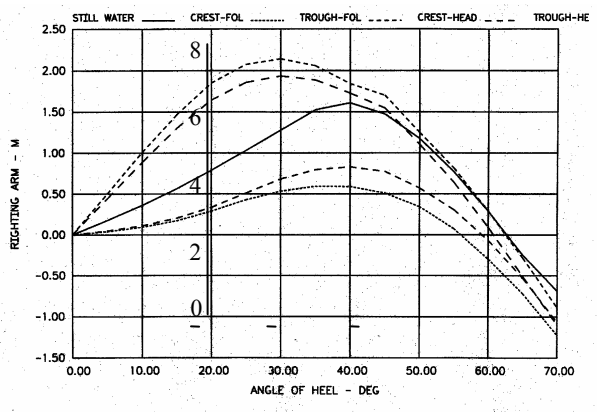

Figure 10. C11 Stability in waves by static approach and dynamic assumptions (including heave and pitch)

SUSCEPTIBILITY CRITERIA

Mathieu Equation

Consider a single degree of freedom equation for roll motion in head seas, taking into account the changing *GM* due to wave encounter.

$$\ddot{\phi} + 2\delta\dot{\phi} + \frac{W \cdot GM(t)}{I_x + A_{44}}\phi = 0 \qquad (9)$$

Here, δ is the linear (or linearized) damping coefficient, W is the weight displacement of a ship, I_x is the transversal moment of inertia, and A_{44} is the added mass in roll.

The variation of *GM* with time may result in parametric resonance. To check if this is possible, the roll equation (9) must be transformed to the form of a Mathieu equation in order to use the Ince-Strutt diagram to examine the properties of the solutions. To do this, we first assume that *GM* changes sinusoidally with time in waves:

$$GM(t) = GM_m + GM_a \cos(\omega t) \qquad (10)$$

Here, GM_m is a mean value of the *GM*. GM_a is the amplitude of the *GM* changes in waves.

$$GM_a = 0.5\left(GM_{\max} - GM_{\min}\right) \tag{11}$$

$$GM_m = 0.5\left(GM_{\max} + GM_{\min}\right) \tag{12}$$

Here, GM_{max} and GM_{min} are maximal and minimal values of metacentric height for a number of wave crest positions along the ship hull, respectively, determined using any appropriate method, including, but not limited to, those described above.

The sinusoidal expression for changes of the *GM* value in waves permits the use of the Mathieu equation, but it is only an approximation. Individual calculation of the *GM* values for successive instantaneous wave positions along the ship gives a more realistic picture. Figure 11 shows the changing values of the *GM* as the wave passes vs. the approximation (10). As can be seen from this figure, the minimum of the true curve is shallower, while the maximum is sharper in comparison with the approximation in (10). The true curve is also shifted a bit, and its amplitude is larger, but these discrepancies are compensated by taking extreme values of the true curve of *GM* instead of *GM* calculated for in wave crest and trough amidships.

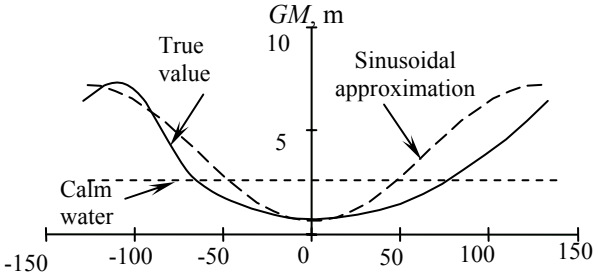

Figure 11. True *GM* values in waves vs. sinusoidal approximation

Substitution of definition (10) into the roll equation (9) yields:

$$\ddot{\phi} + 2\delta\dot{\phi} + \left(\omega_m^2 + \omega_a^2 \cos(\omega t)\right)\cdot \phi = 0 \tag{13}$$

Here:

$$\omega_m = \sqrt{\frac{W \cdot GM_m}{I_x + A_{44}}}; \quad \omega_a = \sqrt{\frac{W \cdot GM_a}{I_x + A_{44}}} \tag{14}$$

In order to transform (13) into the standard form of the Mathieu equation, we introduce dimensionless time:

$$\tau = \omega t \quad \Rightarrow \quad t = \frac{\tau}{\omega} \tag{15}$$

If we now substitute (15) into equation (13) and divide both parts by square of the wave frequency ω^2, we obtain the dimensionless form:

$$\frac{d^2\phi}{d\tau^2} + 2\mu\frac{d\phi}{d\tau} + \left(\overline{\omega}_m^2 + \overline{\omega}_a^2 \cos(\tau)\right)\cdot \phi = 0 \tag{16}$$

Here, the coefficients of equation (16) are the dimensionless quantities:

$$\mu = \frac{\delta}{\omega}; \quad \overline{\omega}_m = \frac{\omega_m}{\omega}; \quad \overline{\omega}_a = \frac{\omega_a}{\omega} \tag{17}$$

The next substitution gets rid of damping:

$$\phi(\tau) = x(\tau)\cdot \exp\left(-\mu\tau\right) \tag{18}$$

This finally expresses roll in the form of a Mathieu equation:

$$\frac{d^2x}{d\tau^2} + \left(p + q\cos(\tau)\right)\cdot x = 0 \tag{19}$$

Here:

$$p = \left(\overline{\omega}_m^2 - \mu^2\right); \quad q = \overline{\omega}_a^2 \tag{20}$$

Bounded and Unbounded Solutions of the Mathieu Equation (Ince-Strutt Diagram)

As is well known, the Mathieu equation (19) may have two types of solutions: bounded (Figure 12) and unbounded, commonly referred as "unstable" (Figure 13).

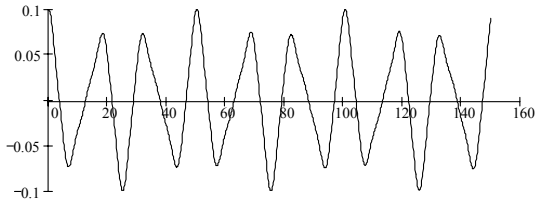

Figure 12. Bounded solution of the Mathieu equation $p = 0.1; q = 0.2$

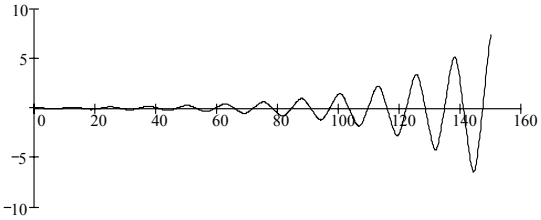

Figure 13. Unbounded solution of the Mathieu equation $p = 0.15; q = 0.2$

Whether a solution is bounded or unbounded depends on the combination of coefficients *p* and *q*. The combinations of *p* and *q* values that correspond to a bounded or unbounded solution can be graphed in a figure that is known as the Ince-Strutt diagram, depicted in Figure 14. The shaded areas correspond to the bounded solution and the unshaded areas to the unbounded solution.

The unshaded areas, identified with Roman numbers in Figure 14, correspond to the unbounded solution and have shapes of curved triangles. Each such triangle touches the p-axis and, with an increase of *q*, becomes wider. The areas with the smaller *p*-intercept grow in width faster; thus we see at the level *q*=2, the first unshaded area is the widest.

The parameter p is seen, in equations (17) and (20), to be equal to the square of ratio of natural and excitation frequencies. The parameter q reflects the level of GM change in waves, expressed as the square of the frequency ratio, as can be seen in equations (11), (15), (17) and (20). Therefore, the parameter q plays the role of an amplitude of parametric excitation. As a result, the entire Ince-Strutt diagram can be considered in terms of the amplitude of parametric excitation vs. the square of non-dimensional frequency.

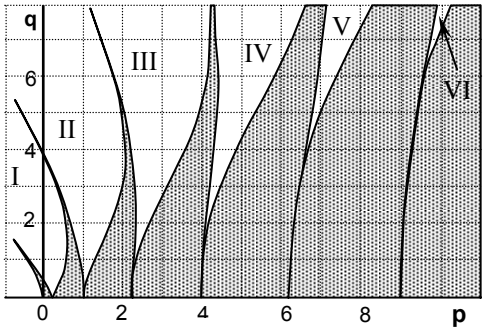

Figure 14. Ince-Strutt diagram

It is also customary to refer to the unshaded areas as instability zones, so we see that the unbounded solution shown in Figure 13 belongs to the first instability zone

The first instability zone intersects the axis exactly at $p = 0.25$, which corresponds to the frequency ratio of 2, so the excitation frequency is twice the natural roll frequency at this point. The unbounded motion belonging to this zone is commonly referred to as the principal parametric resonance.

The second instability zone intersects the axis at $p = 1$, where the excitation frequency is equal to the natural roll frequency. Unbounded solutions belonging to this zone are defined as the fundamental parametric resonance.

The frequency range for the fundamental parametric resonance is smaller [Sanchez and Nayfeh, 1990] than the range for the principal parametric resonance, since the first zone is wider. Also, according to [France, *et al.*, 2003], only the principal parametric regimes were identified during analysis of extreme ship motion of the C11 container carrier. In the following, only the principal parametric resonance will be considered.

Approximations to the Ince-Strutt Diagram

[Stoker, 1950] gives the following linear approximations for the boundaries of the first instability zone of the Ince-Strutt diagram:

$$p_{b1} = \frac{1}{4} - \frac{q}{2} \quad p_{b2} = \frac{1}{4} + \frac{q}{2} \tag{21}$$

Higher order approximations are available from [Hayashi, 1953] transformed for the Mathieu equation (19):

$$p_{b1} = \frac{1}{4} - \frac{q}{2} - \frac{q^2}{8} + \frac{q^3}{32} - \frac{1}{3}\cdot\frac{q^4}{128} + \ldots \tag{22}$$

$$p_{b2} = \frac{1}{4} + \frac{q}{2} - \frac{q^2}{8} - \frac{q^3}{32} - \frac{1}{3}\cdot\frac{q^4}{128} + \ldots \tag{23}$$

Both approximations for the first instability zone are shown in Figure 15.

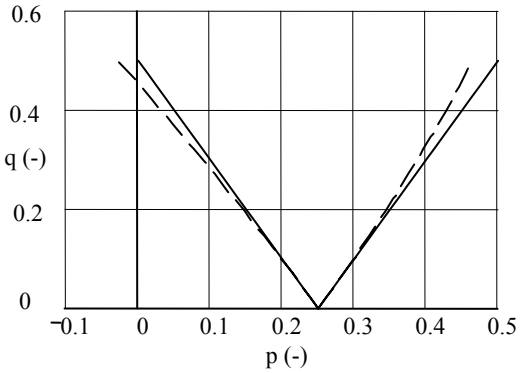

Figure 15. Linear (solid) and high-order (dashed) approximations for the boundary of the first instability zone

Threshold Problem

The Mathieu equation (19) has a periodic bounded solution since the damping was excluded by the substitution (18). It means that the corresponding roll $\phi(\tau)$ decays with the damping decrement μ if $x(\tau)$ is a periodical solution of the Mathieu equation, as shown in Figure 12.

An unbounded solution of the Mathieu equation $x(\tau)$ (as in Figure 13), does not necessarily mean that rolling will be unbounded because the exponential term $\exp(-\mu\tau)$ might undo the effect of boundlessness by damping the solution back to a decaying form.

It also means that there is a threshold value for roll damping for each pair of Mathieu parameters p and q. If roll damping is less than the threshold value, roll will be unbounded as the solution of the Mathieu equation. If the roll damping is larger than the threshold, roll is still bounded, even if the Mathieu equation is unbounded. The increment of the Mathieu solution is not enough to overcome decrement of roll damping. In addition, it is also means that with linear damping, the instability zone is narrower and requires some finite value of GM variations even at p=1/4; i.e., it does not touch the axis.

To calculate this threshold, it is necessary to find a way to express the increment of the unbounded solution of the Mathieu equation. The problem is that solution of the Mathieu equation cannot be expressed in terms of elementary functions. However, there are known expansions for periodical solutions of the Mathieu equation corresponding to the boundary between "stable" and "unstable" zones, known as Mathieu functions. Based on these functions and following [Hayashi, 1953], the threshold value can be presented as:

$$\mu_T = \frac{1}{2}q\left(1-\frac{3}{16}q\right)\times \sqrt{1-\left(\frac{q^2-16+\sqrt{q^4+352q^2+1024p}}{16q}\right)^2} \qquad (24)$$

Structure of Susceptibility Criteria

Summarizing the consideration of roll equation with changing *GM* (9) and the Mathieu equation (19), the Susceptibility Criteria for parametric roll must consist of two conditions:

- Frequency condition: frequency of parametric excitation, i.e., the encounter wave frequency, should be about twice the natural roll frequency. This condition can be formulated in terms of the Mathieu parameters p and q: such that points defined by these parameters should belong to an instability zone on the Ince-Strutt diagram.
- Damping threshold condition: roll damping should be below the damping threshold.

Since both parts of the criteria are based on approximations assuming $|q|$ is small, the above conditions should be tested against the real values of q and p with numerical solution of the roll equation (9) and the Mathieu equation (19).

Frequency Condition of Susceptibility Criteria

As can be seen in Figure 14, the nonlinear approximation slightly shifts both boundaries to the left. It then would be conservative, to use the nonlinear approximation for the left boundary and the linear approximation for the right one. The frequency condition can then be formulated as:

$$\frac{1}{4}-\frac{q}{2}-\frac{q^2}{8}+\frac{q^3}{32}-\frac{1}{3}\cdot\frac{q^4}{128}\le p\le\frac{1}{4}+\frac{q}{2} \qquad (25)$$

The Mathieu parameters p and q are to be calculated with formulae (11), (12), (16), and (29).

Numerical results based on the simplified method (see Table 3 for stability in waves) and EUREKA calculations (see Table 4 for stability in waves) are given in Tables 5 and 6, respectively. The points on the Ince-Strutt diagram are given in Figure 16.

The well known approximate formula was used for the relationship between *GM* value and roll natural frequency where *GM* and B are in meters.

$$\omega_\phi = \frac{2\pi}{T_\phi} = \frac{2\pi\sqrt{GM}}{0.8B} \qquad (26)$$

If we compare results from applying the frequency criterion based on stability computed in longitudinal waves using the simplified method and computed using EUREKA, the simplified method produces slightly more conservative results for the same hull speed and wave.

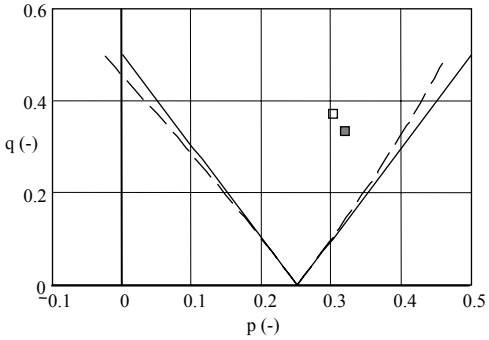

Figure 16. Ince-Strutt diagram for simplified method (open) and EUREKA (solid) (approximations for the boundary of the first instability zone: linear – solid and high-order – dashed)

Table 5. Frequency condition of Susceptibility Criteria (simplified method)

GM value in calm water, m	2.47
Minimal *GM* value, m	0.758
Maximal *GM* value, m	7.59
Natural frequency in calm water, rad/s	0.309
Natural period in calm water T_0, s	20.33
Amplitude of parametric excitation, rad/s	0.363
Accepted ship speed, kn	25.8
Encounter frequency, rad/s	0.803
Encounter period, s	7.82
Accepted non-dimensional damping μ	0.05
Mathieu parameter *p*	0.25
Mathieu parameter *q*	0.2
Frequency condition of Susceptibility Criteria (24)	Yes

Table 6. Frequency condition of Susceptibility Criteria (EUREKA)

GM value in calm water, m	2.58
GM value in wave crest, m	0.87
GM value in wave trough, m	6.58
Natural frequency in calm water ω_0, rad/s	0.332
Natural period in calm water T_0, s	19.922
Amplitude of parametric excitation, rad/s	0.315
Accepted ship speed, kn	22.14
Encounter frequency, rad/s	0.758
Encounter period, s	8.29
Accepted non-dimensional damping μ	0.05
Mathieu parameter *p*	0.19
Mathieu parameter *q*	0.25
Frequency condition of Susceptibility Criteria (24)	Yes

Damping Threshold Condition of Susceptibility Criteria

Formula (25) is supposed to yield a value for the dimpling threshold of the Mathieu equation solution if $|q|$ is sufficiently small.

Here, the damping μ is set slightly greater than the damping threshold by 0.5% in order to be just above the expected threshold. The dimensionless frequencies $\overline{\omega}_m$ and $\overline{\omega}_a$ were set based on the calculation results with the simplified method: to be $\overline{\omega}_m = 0.558$ $\overline{\omega}_a = 0.609$, resulting in the time history shown in Figure 17. Similar results based on EUREKA calculations are shown in Figure 18.

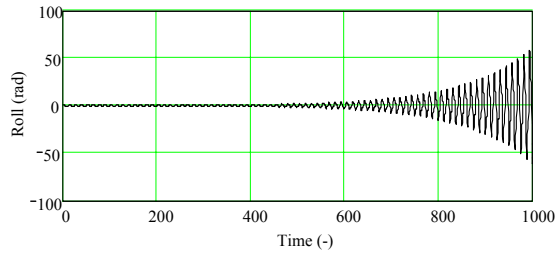

Figure 17. Numerical solution of roll equation (9) with $\overline{\omega}_m = 0.558$ $\overline{\omega}_a = 0.609$ and damping set to damping threshold with formula (32) μ_T=0.1559 (data are based on simplified method)

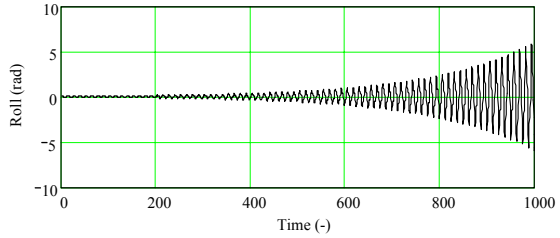

Figure 18. Numerical solution of roll equation (9) with $\overline{\omega}_m = 0.574$ $\overline{\omega}_a = 0.581$ and damping set to damping threshold with formula (32) μ_T=0.132 (data are based on EUREKA)

As can be clearly seen from both Figures 17 and 18, the threshold damping is underestimated by formula (24). The error is probably caused by the assumption that q is small, so formula (24) needs calibration for values of the Mathieu parameter q that are typical of containerships.

The calibration procedure consisted of a series of numerical integrations of the roll equation (9) with different combinations of the dimensionless frequencies $\overline{\omega}_m$ and $\overline{\omega}_a$. Damping was initially set equal to the threshold according to equation (24) and then was increased until the solution became bounded. The correction coefficient is searched in the form:

$$f(\overline{\omega}_a, \overline{\omega}_m) = a_1\overline{\omega}_a + a_2\overline{\omega}_m + a_3 \tag{27}$$

Coefficients a_1, a_2, and a_3 are found by a three-dimensional linear regression based on numerical integration results. The result is as follows:

$$f(\overline{\omega}_a, \overline{\omega}_m) = 1.002\overline{\omega}_a + 0.16\overline{\omega}_m - 0.276 \tag{28}$$

In order to get the correction coefficient, unity should be added to (28). A safety margin of 2% also needs to be included to reduce the error on the dangerous side:

$$k = 1.002\overline{\omega}_a + 0.16\overline{\omega}_m - 0.744 \tag{29}$$

The coefficient k defined by formula (29) is intended to correct the error in the damping threshold and further to appear as coefficient k_3; see formulae (30) and (32) below.

The final form of the damping threshold coefficient is given in equation (30):

$$\mu\frac{\omega_0}{\omega_E} < 0.5 \cdot q \cdot k_1 \cdot k_2\sqrt{1-k_3^2} \tag{30}$$

Here the coefficients k_1, k_2 and k_3 are calculated with the following formulae:

$$k_1 = 1 - 0.1875 \cdot q^2 \tag{31}$$

$$k_2 = 1.002p + 0.16q + 0.759 \tag{32}$$

$$k_3 = \frac{q^2 - 16 + \sqrt{q^4 + 352q^2 + 1024p}}{16q} \tag{33}$$

Sample numerical results based on both the simplified method and EUREKA are summarized in Table 7.

Table 7. Damping threshold condition of Susceptibility Criteria

Value	Simplified method	EUREKA
Mathieu parameter p	0.249	0.249
Mathieu parameter q	0.20	0.19
Damping threshold μ_T	0.208	0.220

Comparing numerical results for the damping threshold based on the simplified method for stability variation in longitudinal waves and on the program EUREKA, it should be noted that the EUREKA–based calculation yields a smaller value for the threshold. This comparison is in line with the previous one, made on the frequency condition of the Susceptibility Criteria. The simplified method gives more conservative values.

Choice of Forward Speed for Susceptibility Criteria

While wave length affects stability changes for the given ship geometry and wave height, the encounter frequency, ω_e is another major factor in the development of parametric roll. Equation (34) gives the encounter frequency in head seas,

$$\omega_e = \omega_w + \frac{\omega_w^2}{g}V \tag{34}$$

The relationship between wave frequency and wave length in deep water is

$$\omega_w = \sqrt{\frac{2\pi g}{\lambda}} \tag{35}$$

Parametric roll is most likely to develop when the encounter frequency is about twice the natural roll frequency while in a wave length about equal to the ship length. We note that the roll natural frequency in waves may be different from that in calm water because the average value of the *GM* differs somewhat from that in calm water as may be seen in Figure 11. The ship speed for this condition of parametric resonance is given by equation (36).

$$V_{pr} = \frac{g(2\omega_m - \omega_w)}{\omega_w^2} \tag{36}$$

Negative speed calculated with (36) means that parametric roll may be expected in following waves. If a ship is capable of the speed given by (36), the susceptibility check should be carried out with this speed (36) and with the wave length equal to ship length. If a ship is not capable of the speed V_{pr}, the check has to be done for the service speed V_S, closest to this speed given by (36). In most cases, this will be the maximum service speed:

$$V = V_s \quad \text{if} \quad V_{pr} > V_S \tag{37}$$

$$V = V_{pr} \quad \text{if} \quad V_{pr} < V_S \tag{38}$$

A negative susceptibility check with the speed (37), however, should be reconsidered since there might be another wave length perhaps with a smaller change of stability but with a more critical encounter frequency. Assuming the ship moves with the speed V_S, it is possible to find a wave length meeting the condition $\omega_e = 2\omega_m$, and this is given in equation (39):

$$\omega_w + \frac{\omega_w^2}{g} V_S - 2\omega_m = 0 \tag{39}$$

Formula (47) is seen to be a quadratic equation, having the following solutions:

$$\omega_{w1,2} = \frac{1}{2V_S}\left(-g \pm \sqrt{g^2 + 8V_S\omega_m g}\right) \tag{40}$$

One solution is always positive and another is always negative. Since only the head seas case is considered here, we use just the plus sign.

$$\omega_w = \frac{\sqrt{g\left(g + 8V_S\omega_m\right)} - g}{2V_S} \tag{41}$$

The new wave length is:

$$\lambda = \frac{2\pi}{k} = \frac{2\pi g}{\omega_W^2} = \frac{8\pi g V_S^2}{\left(\sqrt{g\left(g + 8V_S\omega_m\right)} - g\right)^2} \tag{42}$$

VERIFICATION OF SUSCEPTIBILITY CRITERIA

Simulation Tools

Verification of the Susceptibility Criteria was carried out with the LAMP time-domain simulation software.

LAMP – the Large Amplitude Motions Program – uses a time stepping approach in which all of the forces and moments acting on the ship, including those due to the wave-body interaction, appendages, control systems, and green-water, are computed at each time step and the 6-DOF equations of motions are integrated in the time-domain using a 4th-order Runge-Kutta algorithm. In addition to motions, LAMP also computes main girder loads using a rigid or elastic beam model and includes an interface for developing Finite-Element load data sets from the 3-D pressure distribution [Weems, *et al.,* 1998].

The central part of the LAMP System is the 3-D solution of the wave-body interaction problem in the time-domain [Lin and Yue, 1990, 1993]. A 3-D disturbance velocity potential is computed by solving an initial boundary value problem using a potential flow "panel" method. A combined body boundary condition is imposed that incorporates the effects of forward speed, ship motion (radiation), and the scattering of the incident wave (diffraction). The potential is computed using a hybrid singularity model that uses both transient Green functions and Rankine sources [Lin *et al.,* 1999]. Once the velocity potential is computed, Bernoulli's equation can then be used to compute the hull pressure distribution, including the second-order velocity terms

A number of LAMP validation studies have been performed, including an extensive series of calculation for the U.S. Navy CG-47 class cruiser in storm sea conditions (*e.g.*, [Weems, *et al.*, 1998]). These studies have been instrumental in validating both of LAMP's "body-nonlinear" and "approximate body-nonlinear" approaches to predicting the nonlinear behavior of bending moments for flared-bow ships in extreme sea conditions. A description of the latest development and most recent LAMP applications can be found in [Shin, *et al.,* 2003].

For the purpose of validating the parametric roll criteria, LAMP-2 was used. In this version of LAMP the hydrostatic and Froude-Krylov forces were calculated on the instantaneous submerged body, while the mean waterline was used for the computations of radiation and diffraction forces.

Basic Verification

The first set of verification was performed to make sure that Susceptibility Criteria were capable of indicating parametric resonance. In order to verify such capability, the criteria should be applied for the case when existence of parametric roll is certain, such as conditions from [France, *et al.,* 2003]. One such case involving the C11-class container carrier at a speed of 10 knots in a wave height of 8.4 m and a wave circular frequency of 0.44 rad/s was successfully reproduced in [Belenky, *et al.*,

2003]. The model geometry is shown in Figure 19 and panelization in Figure 20. Time histories of the simulated motions are shown in Figures 21-23.

Figure 21 contains a typical picture of the development of parametric resonance. Here, a significant rise of roll amplitude is accompanied by a small decrease in heave (Figure 22) and a very small decrease in pitch (Figure 23).

Numerical results of the application of the Susceptibility Criteria are summarized in Table 8 and shown in Figure 24.

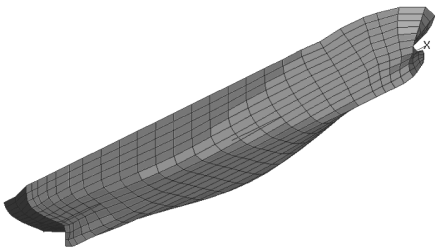

Figure 19. Geometry of C11 class container carrier

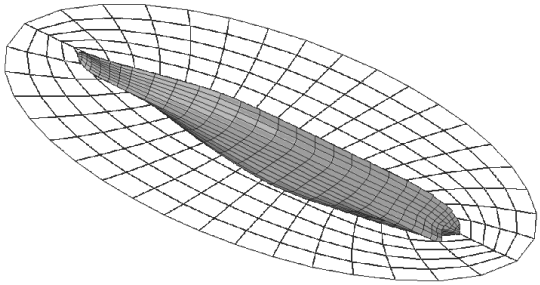

Figure 20. Panel model of C11 class container carrier

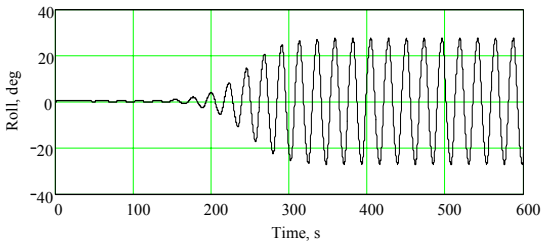

Figure 21. Development of parametric roll in regular waves (wave amplitude 4.2 m, frequency 0.44 s^{-1}, speed 10 knots)

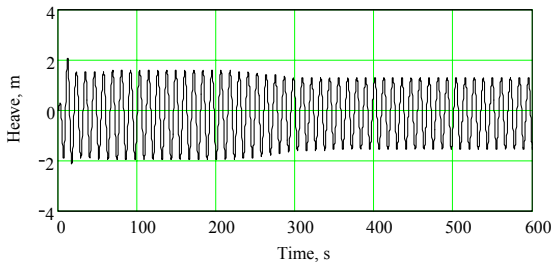

Figure 22. Heave motions accompanying parametric roll in regular waves

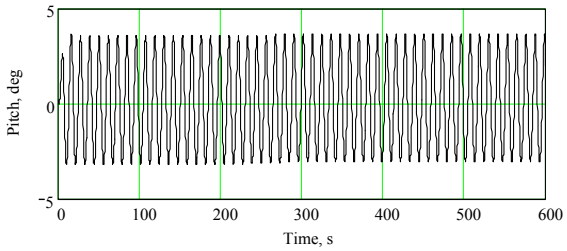

Figure 23. Pitch motions accompanying to parametric roll in regular waves

Table 8. Basic verification of Susceptibility Criteria

GM value in calm water, m	2.52
GM value in wave crest, m	1.30
GM value in wave trough, m	4.64
Natural frequency in calm water ω_0, rad/s	0.312
Natural period in calm water T_0, s	20.158
Amplitude of parametric excitation, ω_a, rad/s	0.254
Accepted ship speed, kn	10
Encounter frequency, rad/s	0.55
Encounter period, s	11.43
Accepted non-dimensional damping μ	0.05
Mathieu parameter *p*	0.319
Mathieu parameter *q*	0.213
Frequency condition of Susceptibility Criteria (25)	Satisfied
Damping threshold value (30)	0.087
Damping threshold condition of Susceptibility Criteria	Satisfied

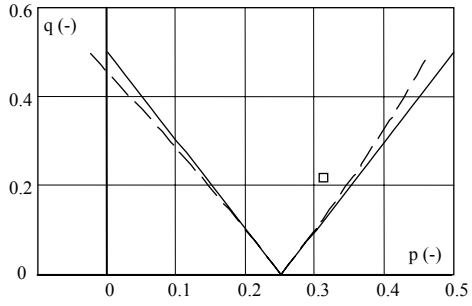

Figure 24. Basic verification of Susceptibility Criteria: (wave amplitude 4.2 m, frequency 0.44 s^{-1}, speed 10 kn)

Boundary Verification

Susceptibility Criteria establish certain boundaries for Mathieu parameters. Here, parametric resonance is possible. Further verification involves testing if the criteria are capable of correctly distinguishing whether conditions that lead to the parametric resonance are possible from those that do not. In order to facilitate such testing, a series of LAMP simulations were carried out with variations of wave length, while keeping all other characteristics exactly the same. The results are summarized in Table 9 and shown in Figure 25.

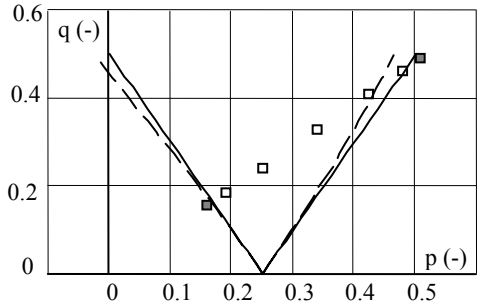

Figure 25. Boundary verification wave height 13.1 m, solid squares – no parametric roll

As can be seen both from Table 9 and Figure 25, Susceptibility Criteria provide reasonable boundaries for parametric roll.

Sensitivity Verification

In order to perform an overall check of sensitivity for the Susceptibility Criteria, data for a 300,000-ton deadweight tanker were next used. There is no evidence that large tankers are susceptible to parametric resonance, despite the fact that tankers of similar size have been in operation since the early 1970s. The full form with limited vertical shape changes in combination with relatively slow speed makes parametric roll extremely unlikely for large tankers. Principal data for the tanker is given in Table 10 and its body plan are shown in Figure 26, while calculations are summarized in Tables 11 and 12

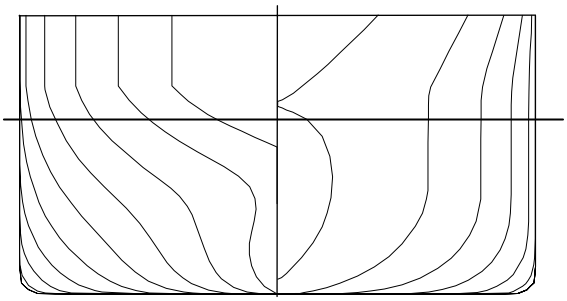

Figure 26. Lines of 300,000-ton tanker

Table 9. Summary of numerical results for Boundary verification wave height 13.1 m, displacement 76,400 ton, EUREKA calculations

Wave freq. rad/s	0.37	0.38	0.40	0.445	0.50	0.56	0.60
Wave length, m	450	426	385	310	246	196	171
GM /wave crest, m	1.00	1.00	1.00	1.00	1.00	1.00	1.00
GM / wave trough , m	5.98	5.98	5.98	5.98	5.98	5.98	5.98
Encounter freq., rad/s	0.442	0.456	0.484	0.55	0.631	0.724	0.789
Mathieu parameter *p*	0.508	0.478	0.424	0.338	0.249	0.189	0.1595
Mathieu parameter *q*	0.491	0.462	0.410	0.327	0.241	0.183	0.154
Damping threshold	0	0	0.05	0.13	0.12	0.0736	0
Damping parameter μ	0.036	0.035	0.033	0.029	0.0250	0.0218	0.0200
Criteria satisfied	No	Yes	Yes	Yes	Yes	Yes	No
Simulation indicates parametric resonance	No	Yes	Yes	Yes	Yes	Yes	No

Table 10. Tanker data

Length BP, m	320.0
Molded Breadth, m	52.0
Depth, m	31.0
KG, m	19.4
Draft	21.0
Displacement, ton	318950

Table 11. Susceptibility Criteria for tanker- first check

Method of calculating stability in waves	**Simpl**	**EUREKA**
GM value in calm water, m	4.3891	4.55
GM value in wave crest, m	4.4201	4.54
GM value in wave trough, m	5.8304	5.80
Natural freq. in calm water ω_0, rad/s	0.3222	0.3222
Natural period in calm water T_0, s	19.5	19.5
Wave frequency, rad/r	0.4389	0.4389
Amp.of parametric excitation, rad/s	0.1268	0.1199
Parametric resonance ship speed, kn	19.86	20.34
Accepted ship speed, kn	12.0	12.0
Encounter frequency, rad/s	0.56	0.56
Encounter period, s	11.22	11.22
Damping parameter μ (with accepted roll damping 5% of critical)	0.0288	0.0288
Mathieu parameter *p*	0.318	0.33
Mathieu parameter *q*	0.0513	0.0458
Frequency condition (32)	No	No
Damping threshold	0	0
Damping threshold condition (37)	No	No

Table 12. Susceptibility Criteria for tanker- second check

Method of calculating of stability in waves	**Simpl.**	**EUREKA**
Param. roll wave length (50), m	262.1	254.6
Param. roll wave freq. (40), rad/s	0.485	0.492
Param. roll wave height, m	13.1	12.7
GM value in calm water, m	4.3891	4.55
GM value in wave crest, m	4.3672	4.52
GM value in wave trough, m	5.316	5.25
Nat. freq. in calm water ω_0, rad/s	0.3222	0.3222
Natural period in calm water T_0, s	19.5	19.5
Amp. of param. excitation, rad/s	0.104	0.0913
Param. resonance ship speed, kn	12.0	12.0
Accepted ship speed, kn	12.0	12.0
Encounter frequency, rad/s	0.6329	0.6444
Encounter period, s	9.928	9.751
Damping parameter μ (with accepted roll damping 5% of critical)	0.025	0.025
Mathieu parameter *p*	0.2494	0.2494
Mathieu parameter *q*	0.0269	0.02
Frequency condition of Susceptibility Criteria (4.49)	Yes	Yes
Damping threshold	0.0136	0.01014
Damping threshold condition of Susceptibility Criteria	No	No

Figure 27 shows Ince-Strutt diagrams for the first and second check of the Susceptibility Criteria using stability computed by the simplified method and by EUREKA, respectively. The first check of Susceptibility Criteria yields a negative frequency condition. The ship was simply too slow and the stability in waves did not change enough to enter the zone of unbounded solution of the Mathieu equation. The second check indicated a positive frequency condition of the Susceptibility Criteria, which was expected because the speed was especially set up to meet the frequency of parametric resonance. However, the damping threshold condition was not satisfied by the second check, which ruled out the possibility of parametric roll.

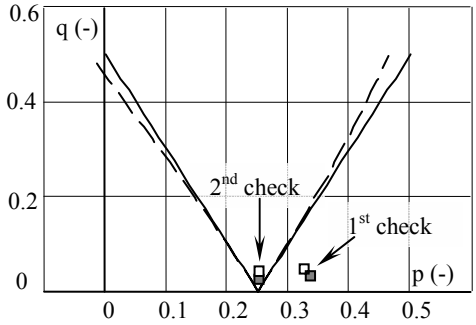

Figure 27. Ince-Strutt diagram for the tanker: first and second check. (open– simplified method, solid-EUREKA)

To confirm the absence of parametric roll for the tanker, LAMP simulations were carried out in conditions exactly corresponding to those of the first and second susceptibility checks. Geometry and panelization are presented in Figures 28 and 29, simulation results (roll, heave and pitch) for the 1st check condition (wave length equal to ship length) in Figure 30, and simulation results for the 2nd check (speed is chosen to set parametric resonance condition for encounter frequency) in Figure 31.

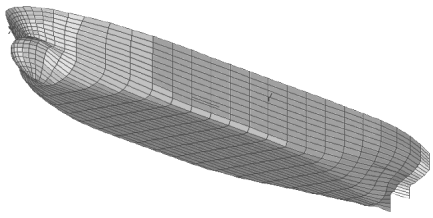

Figure 28. Geometry of the 300,000 ton tanker

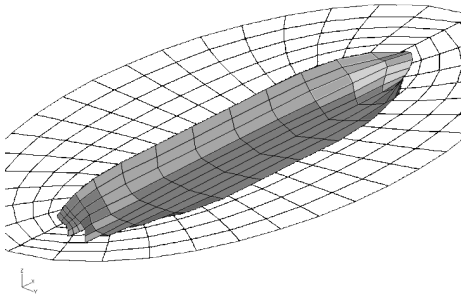

Figure 29. Panelization for the 300,000 ton tanker

These LAMP simulations confirmed the fact that large tankers are not susceptible to parametric roll – a fact, as noted before, that was well known from operational experience. At the same time, these simulations showed good agreement with the Susceptibility Criteria, which came up negative for the 300,000-ton tanker. The latter completes the sensitivity check of the Susceptibility Criteria.

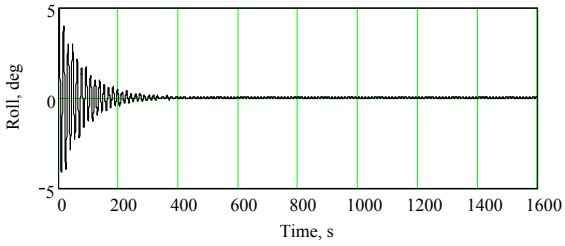

Figure 30. Roll motion: 1st check wave length 320 m, speed 12 kn

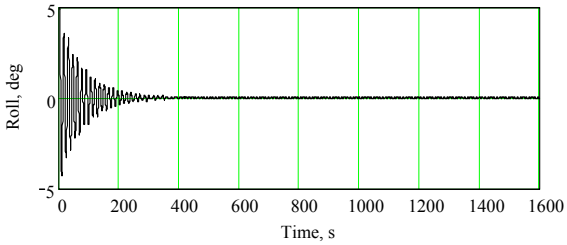

Figure 31. Roll motion: 2nd check wave length 254.6 m, speed 12 kn

AMPLITUDE OF PARAMETRIC ROLL IN REGULAR WAVES

Influence of Nonlinearity

Applicability of any solution based on the Mathieu equation is limited because it is linear: it can indicate conditions when parametric roll can be generated, but it is unable to predict amplitude. Such an answer is not enough for engineering practice: the solution must determine how large the parametric roll might develop if conditions satisfy the Susceptibility Criteria (25) and (30). Once parametric roll is indicated, the solution of the Mathieu equation is unbounded and grows indefinitely. In the real world, however, parametric roll is limited to a finite, though sometimes large, amplitude, as shown in Figure 21. It is known that nonlinear terms in the rolling equation stabilize parametric rolling. The two major nonlinear terms in the one-degree-of-freedom rolling equation are the restoring and damping terms.

Although the actions of both terms have similar results in limiting parametric roll, the physics of their actions are different. Nonlinearity of the *GZ* curve at large angles of heel leads to a significant change of the effective *spring constant with amplitude*, and, therefore, of natural roll frequency. Change of the natural frequency takes the system out of the instability zone of the Ince-Strutt diagram. This means that the input of additional energy ceases once the roll achieves a certain angle. As a result, an energy balance is established and roll stabilizes itself at a certain amplitude provided that capsizing does not occur.

Nonlinear damping has a tendency to increase with roll velocity, so sooner or later it will grow above the damping threshold. Then, the system dissipates more energy than is input from parametric excitation, which also leads to stabilization of the roll amplitude.

It is also known (see, for example [Bulian, *et al.,* 2003]) that the nonlinearity of the *GZ* curve is more important in the stabilization of parametric roll than nonlinear damping.

Asymptotic Methods

Based on the above, rolling equation (13) is re-written with only the restoring nonlinearity meanwhile retaining only the linearized damping coefficient δ:

$$\ddot{\phi} + 2\delta\dot{\phi} + \omega_m^2\left(1 + a_p\cos(\omega_e t)\right)\cdot\phi - a_3\phi^3 = 0 \qquad (43)$$

Here a_3 is a third power coefficient used to approximate the nonlinear *GZ* curve, $a_p = \omega_a^2/\omega_m^2$. As an approximation we take into account the wave influence on the *GM*-related term only. Here we use the solution from [Sanchez and Nayfeh, 1990] obtained by applying the method of multiple scales [Nayfeh, 1981]. The solution is searched around a frequency that is about twice the natural frequency:

$$\frac{1}{4}\omega_e^2 = \omega_m^2 + \varepsilon\cdot\sigma \qquad (44)$$

Here ε is a small value (bookkeeping parameter) and σ is a tuning parameter. The solution is searched in the form:

$$\phi(t) = \phi_a\sin(\omega_e t + \beta) \qquad (45)$$

Using the method of multiple scales, the steady-state amplitude and phase can be expressed as:

$$\beta = \frac{1}{2}\arcsin\left(\frac{8\delta}{\omega_e\overline{\omega}_a}\right) \qquad (46)$$

$$\phi_a = \frac{\sqrt{\omega_e^2 - 4\omega_m^2 - 0.5\omega_e\sqrt{\omega_e^2 a_p^2 - 64\delta^2}}}{\sqrt{3a_3}} \qquad (47)$$

Formula (47) demonstrates how the nonlinearity affects the parametric roll amplitude since the amplitude tends to infinity as the third-power coefficient a_3 decreases:

$$\lim_{a_3\to 0}\phi_a = \infty \qquad (48)$$

A detailed description of the solution, as well as a sample application of the multiple scales method, is also available from [Belenky and Sevastianov, 2003]. Other analytical methods also can be applied; see [Umeda, *et al.,* 2003] and [Neves, *et al.*, 2003].

Sample Calculations with Asymptotic Formula

Although the formula for the amplitude of parametric roll (47) is simple, its practical application for a real ship encounters difficulties. The roll equation (43), which is a background for formula (47), contains an approximation

for the *GZ* curve using a third power polynomial. However, this does not provide sufficient accuracy for predicting the parametric roll amplitude in the case of a real ship. Figure 32 shows a set of *GZ* curves calculated with EUREKA for a number of positions of the wave crest along the ship hull. This figure includes a *GZ* curve averaged over all wave positions and a calm water *GZ* curve is also depicted for reference. Figure 33 contains the result of approximating the average *GZ* curve using the method of least squares together with a third order polynomial. The averaged *GZ* curve obtained in this way is shown in Figures 32 and 33:

$$GZ(\phi) = A_1\phi - A_3\phi^3 \qquad (49)$$

The following values were obtained as a result of the mean square curve fitting:

$A_1 = 3.997\,m$; $A_3 = 2.839\,m$

Other numerical results are given in Table 13.

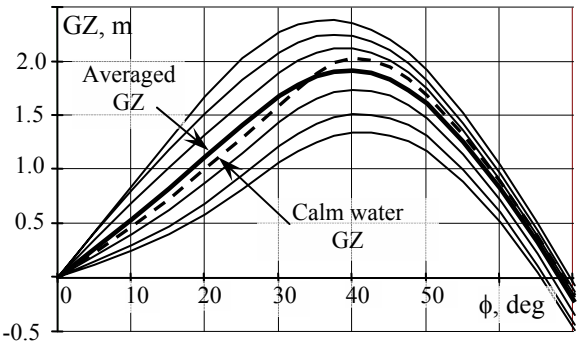

Figure 32. *GZ* curves calculated for different positions of the wave crest along ship length

Table 13. Amplitude of Parametric Roll with Asymptotic Formula

Wave length, λ, m	262
Wave amplitude, m	4.2
GM value based on approximated *GZ* curve, m	3.997
Roll frequency based on approximated *GZ* curve, ω_m rad /s	0.393
Third power coefficient, expressed in terms of angular accelerations a_3, $1/s^2$	0.109
Amplitude of *GM* value changes in wave (amplitude of parametric excitation), m	1.945
Non-dimensional amplitude of parametric excitation, a_p	0.487
Incident wave frequency ω, rad/s	0.482
Forward speed, kn	10.0
Encounter wave frequency, ω_e, rad/s	0.604
Amplitude of parametric roll, ϕ_a deg	56.47

The case above is slightly different from that on Figure 21 in the wave frequency, but the wave length equals to ship length. The roll time history is shown in Figure 34.

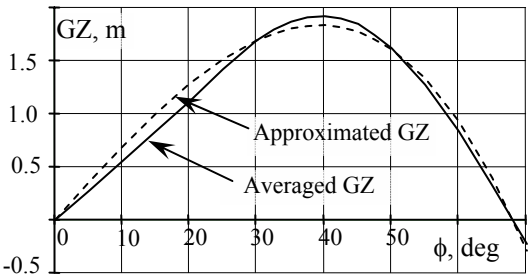

Figure 33. Approximation of the averaged *GZ* curve with third power polynomial

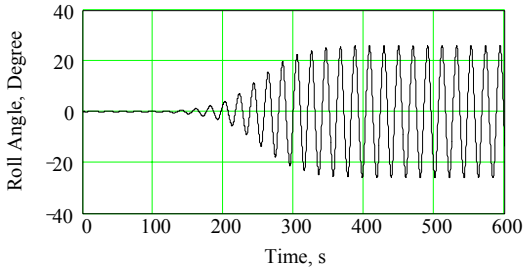

Figure 34. Development of parametric roll in regular waves (wave amplitude 4.2 m, frequency 0.485 s^{-1}, speed 10 knots)

The amplitude of parametric roll obtained with the LAMP simulation is 26.04 degrees. This is significantly different compared with the result of the asymptotic formula. As noted above, the nonlinearity of the *GZ* curve is responsible for stabilizing the parametric roll, and therefore the difference between the actual shape and the approximation may be the reason for the difference. Another possible reason is that formula (48) is derived as the first expansion, and this may not be sufficiently accurate.

The results might be improved by using a higher order polynomial for the approximation of the *GZ* curve, and the formula for the amplitude could be derived from the second or higher order expansion. However, the new formulae might be especially complex, requiring solution of a system of nonlinear algebraic equations, so the direct numerical integration of the rolling equation seems to be preferable at this stage.

Numerical Methods

The amplitude of parametric roll may be obtained by numerical integration of the following rolling equation:

$$\ddot{\phi} + 2\delta\dot{\phi} + \omega_m^2 f(\phi, t) = 0 \qquad (50)$$

The restoring term $f(\phi, t)$ has to be obtained by two-dimensional interpolation in a table of calculated values of the *GZ* curve, as shown in Figure 32. First, the series of curves at Figure 32 have to be presented as a surface; see Figure 35. Then, the transition is to be made from wave crest position to time variable:

$$x = V \cdot t - L \cdot floor\left(\frac{V \cdot t}{\lambda}\right) \qquad (51)$$

The numerical function *floor* is defined as the greatest integer number smaller than the argument $(V \cdot t / \lambda)$. Here V is a ship speed relative to incident waves:

$$V = V_S + c \tag{52}$$

Where c is wave celerity:

$$c = \frac{\lambda}{T_w} = 2\pi\omega_W \lambda \tag{53}$$

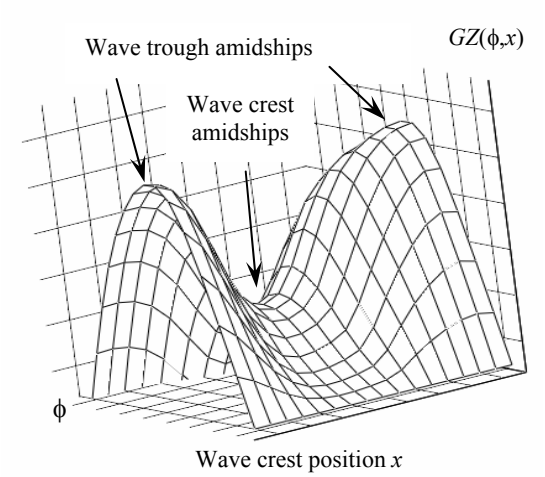

Figure 35. Restoring moment as a function of wave position and roll angle

Using the relationship between wave crest position and time in the form (51) permits the restoring term to be presented as a periodic function of time. Dividing the righting arm by the averaged *GM* value and making it symmetrical with roll angles port and starboard for symmetrical ship geometry and loading conditions, yields

$$f(\phi, t) = \frac{sign(\phi)}{\mathrm{GM_m}} GZ(|\phi|, t) \tag{54}$$

The function *sign(ϕ)* is defined as –1 if the value of roll angle ϕ is negative and defined as +1 if positive. The symbol |ϕ| signifies absolute value. The resulting restoring term is shown in Figure 36.

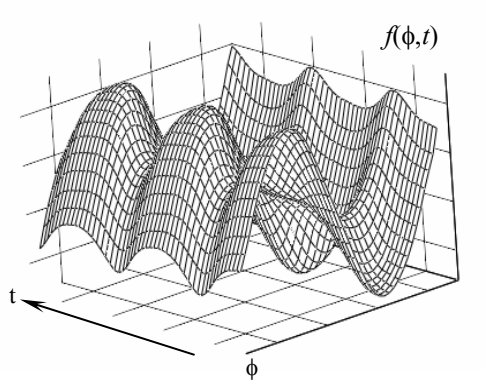

Figure 36. Restoring term as a function of time and roll angle

The result of the integration of equation (50) is shown in Figure 37. The steady state amplitude obtained from this solution equals 31 degrees, which is much closer to the LAMP result than was the asymptotic solution. The above procedure is the basis of the Severity Criterion of parametric roll.

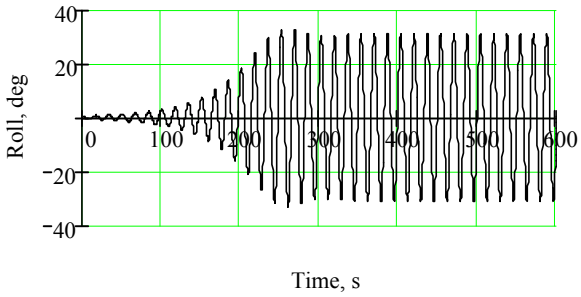

Figure 37. Result of numerical integration of rolling equation (50)

PARAMETRIC ROLL IN IRREGULAR WAVES

Influence of Nonlinearity

Following successful parametric roll simulation with LAMP and FREDYN programs described in [France, *et al.*, 2003], another series of LAMP simulations were specifically aimed at studying the probabilistic characteristics of irregular rolling in the regime of parametric resonance [Belenky, *et al.*, 2003]. As the ultimate goal is an estimate of the risk of parametric roll, it must be clear as to what kind of stochastic process the parametric roll constitutes. The main concern here is the role that nonlinearity plays in the dynamics of parametric roll, since without nonlinearity the parametric oscillations are not bounded. It would be logical to suggest that the dynamical system capable of an adequate description of the parametric roll would be significantly nonlinear.

Nonlinearity of the dynamic system makes description of its response to random excitation more complicated and the greatest concern is ergodicity and distribution.

Ergodicity

Ergodicity is a quality of a stationary stochastic process that is not applicable to a non- stationary process. If the process is ergodic, its statistical characteristics can be evaluated from one realization, provided it is long enough. If the process is not ergodic, we have to consider a statistically significant number of realizations in order to get reliable statistical estimates. Irregular waves in the open sea are known to be ergodic processes within the period of quasi-stationarity, that is, the time when a sea state could be considered constant. It is mathematically proven that if a dynamical system is linear, then its response to ergodic excitation is also ergodic. On the other hand the response of a nonlinear system might be non-ergodic and several realizations would be needed to obtain reliable statistical estimates.

The second series of LAMP simulations for parametric roll in a C11 class containership [Belenky, *et al.*, 2003] was carried out using exactly the same conditions as the first one series [France, *et al.*, 2003].

The second series consisted of 50 realizations generated from the same JONSWAP spectrum, but with a different set of random phases for each realization. Two of the roll response realizations are shown below in Figure 38. The difference between them is quite obvious.

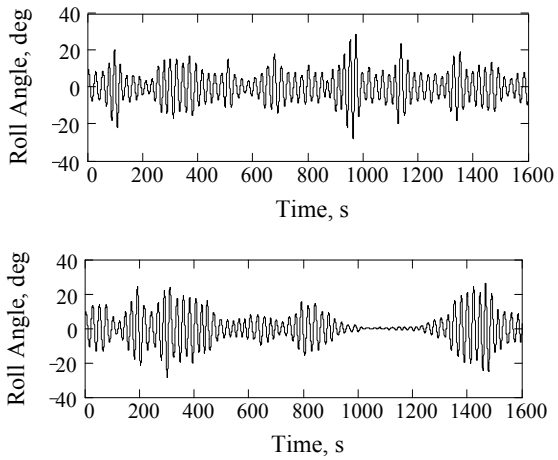

Figure 38. Sample of two parametric realizations

Further statistical analysis indicated the absence of ergodicity of roll, while heave and pitch still can be assumed ergodic, as indicated in Figure 39, where results for roll are shown. Each point there represents roll variance estimates along with 99.73% confidence intervals. It is very clear that these confidence intervals do not overlie one another, which means that the difference between realization estimates is caused by the absence of ergodicity and not by the random error from insufficient statistical data.

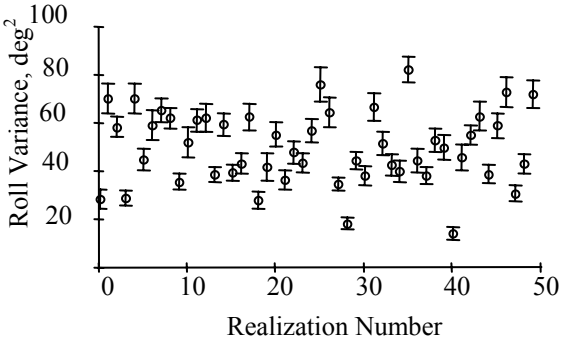

Figure 39. Realization variance estimates and confidence intervals for roll motion [Belenky, *et al.,* 2003]

Probability Distribution

The second problem is related to the probability distribution. The probability distribution of waves in the open sea is usually well described by a Gaussian or normal distribution. Again, it is proven that the response of a linear dynamical system to a Gaussian distribution is also normal while the response of a nonlinear system is not necessarily normal. The distribution of parametric roll was found to be quite different from normal as may be seen in Figure 40. More details of this study are available from [Belenky, *et al.,* 2003].

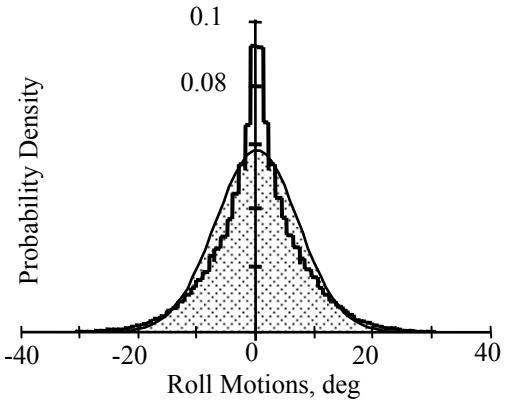

Figure 40. Probability distribution of roll motions [Belenky, *et al.,* 2003].

The above results should be taken into account when planning time domain simulations in irregular seas, since several realizations for the same conditions are necessary. This makes time domain simulation more computationally expensive, but with the present rapid growth in computing speed, this is not a major consideration.

Review of Probabilistic Methods

This section reviews different methods of treating irregular nonlinear roll and examines them for possible application to parametric roll.

As noted above, numerical simulations with LAMP and FREDYN successfully reproduced parametric roll in irregular seas. Therefore, it seems logical to use these instruments for evaluation of the operational risk of parametric roll [Leavdou and Palazzi, 2003]. The approach adopted in the referred paper uses voyage simulation with several environmental conditions as the ships sail from departure to destination ports. An assumption was used that, for a large container ship, parametric roll is the only cause of excessive roll, so any roll angles above 20 degrees are attributed to parametric resonance and included in the statistics to evaluate risk.

With the evident advantage of using the most sophisticated tools, this approach involves significant computational costs. Long roll response realizations needed for the voyage simulations require equally long incident wave realizations. Construction of long wave realizations involves a large frequency set as frequency step determines the statistically representative length of realization. (See [Belenky and Sevastianov, 2003] for more details.) Absence of ergodicity requires repeating the same simulation of a given set of environmental conditions many times, which also adds to computational effort.

Since most of the analytical tools to treat parametric roll, *e.g.*, the Mathieu equation, are available for regular waves, the envelope approach is also a logical choice. If a

stochastic process is stationary and has a Gaussian distribution, it can be presented as:

$$x(t) = A(t)\cos\left(\Phi(t)\right) \tag{55}$$

The amplitude $A(t)$ and phase $\Phi(t)$ are stochastic processes, which could be considered as slowly varying functions in comparison with the process itself, as shown in Figure 41.

If a process has a relatively narrow spectrum, which is acceptable for ocean waves surfaces, presentation (55) can be expressed as:

$$x(t) = A(t)\cos(\omega_a t + \varphi(t)) \tag{56}$$

Where ω_a is a frequency averaged over the spectrum. To ensure that (56) has a desired spectrum, a special filter differential equation is considered in conjunction with the roll equation. Applications for typical sea spectra could be found in [Francescutto and Nabergoj, 1990]. Once the spectrum is defined, the rolling equation together with the filter equation can be solved with any method suitable for deterministic excitation; see samples of application for Duffing's equation [Davies and Rajan, 1988] and roll in beam seas [Francescutto 1991, 1992, 1998]. The method was used for parametric roll and validated against model test; see [Bulian, *et al.*, 2003]

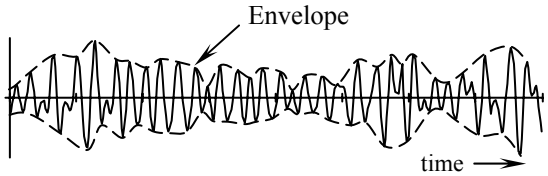

Figure 41. Envelope of stochastic process [Belenky and Sevastianov, 2003]

Another way to replace irregular waves with a regular wave is to use the "effective wave concept. A description is given in [Grim, [1961], also by [Belenky and Sevastianov, 2003]. The concept is illustrated in Figure 42. The idea is that an irregular wave should be replaced by a regular one with the length equal to the length of a ship and its crest or trough situated at the center of gravity. The effective wave concept was used by [Umeda, 1990] and [Umeda and Yamakoshi, 1993] for calculating probability of ship capsizing due to pure loss of stability in quartering seas. A comparison between effective wave concept and direct stability calculations has validated such an approach. Recently, this method was applied to the problem of parametric roll; see [Umeda, *et al.,* 2003].

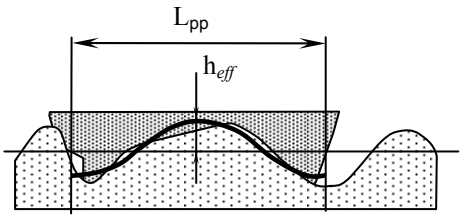

Figure 42. Concept of effective wave [Grim, 1961]

Application of Markov processes is yet another approach used for treatment of parametric roll in irregular seas. A Markov process is defined as a stochastic process, for which the current value depends only on the previous one. This is a simplification in comparison with the general concept of a stochastic process, for which current value depends on all the previous values. As a result, several general solutions are available for a Markov process: there is a known relationship between the probability distribution at the given moment and the previous moment, known as the Fokker-Planck-Kolmogorov (FPK) equation. The probability of reaching the given level also could be solved analytically for many cases. General problems and a review of applying Markov processes for nonlinear roll can be found in [Roberts, 1982]. Applications for parametric roll are described in [Roberts, 1982a] and [Bulian, *et al.*, 2003]. The latter compares the theoretical results with a model test.

As is well known, irregular waves at sea have a group structure, with a group of relative high waves followed by several relatively small waves, as illustrated in Figure 43.

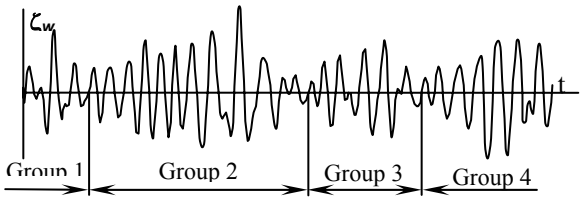

Figure 43. Group Structure of irregular seas [Belenky and Sevastianov, 2003]

Statistics on wave groups are available that can be used for treatment of parametric roll ([Boukhanovsky and Degtyarev, 1996] and [Degtyarev and Boukhanovsky, 2000]). It was found that parametric roll is more likely to occur when ships encounter a long group with a large number of waves. The periods of waves in the group are more important than their height, and a sequence of short groups with similar periods could be very dangerous. A brief review of these results is also available from [Belenky and Sevastianov, 2003].

Choice of Wave Height

The review, above, shows that there is no well-established standard method to evaluate the probability of parametric roll, but there are available options that are worth pursuing in order to develop such a capability in future.

In the meantime, an equivalent design wave can be used in order to assess parametric roll. The length of such a wave is already established as being equal to the ship length to maximize the effect of stability change in waves, but the wave height has to be assigned. This wave height has to be large enough to put parametric excitation above the threshold and still be realistic enough to be encountered during a severe storm. One of the possible ways is to use a wave scatter table, where each combination of averaged zero-crossing wave period T_z

and significant wave height h_s is mapped to statistical frequency or probability estimate of observation.

It is assumed that the design wave length defines the average zero-crossing period and design wave height is equal to significant wave height. Then, it is possible to determine the height using equal statistical frequency. Such statistical frequency in the wave cell was set up to 10^{-5} and the wave scatter table from [IACS 2001] was used. The resulting dependency of the design wave height and wave length was placed in Table 13, which is used in the ABS Guide to determine the height of the design wave for parametric roll assessment. For the lengths between those given in Table 14, linear interpolation is expected to be used. For practical reasons, the wave height should be limited by the freeboard.

Table 14. Choice of Design Wave Height

Wave length λ, m	Wave height h_W, m
50	5.9
100	11.6
150	14.2
200	15.1
250	15.2
300	14.6
350	13.6
400	12.0
450	9.9

CONTROL OF PARAMETRIC ROLL

Since parametric roll, like all parametric oscillations, has an excitation threshold that must be overcome in order for the phenomenon to exist, a natural way to mitigate parametric roll would be to decrease the excitation below the threshold by creating an opposing roll moment. The opposing roll moment could be generated by anti-rolling fins, water motion in tanks, moving mass systems, or rudder deflection and it could be actively controlled or passive.

The study [Lin and Weems, 2002], [Shin, *et al.,* 2003], and [Belenky, *et al.,* 2003] considered a container ship fitted with a passive, U-tube anti-rolling tank. The ship in this study is similar to, but somewhat larger than, the C11-class container ship studied above.

A method for approximating a U-tube type passive anti-roll tank system has been implemented as an optional "plug-in" module in LAMP. The system calculates fluid motion in the U-tube tank and determines the coupled nonlinear forces acting on a floating body in full six degrees of freedom. These forces are added to LAMP's calculation of motion and loads as an external (non-pressure) force. A schematic of the anti-roll tank is shown in Figure 44.

The tank model includes expressions for the shear stress on the tank walls and energy losses in the elbows, but does not account for "sloshing" in the vertical columns themselves. The theoretical description of the model can be found in [Yossef, *et al.*, 2003

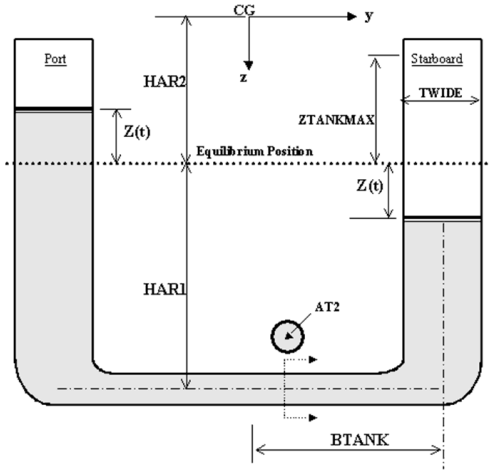

Figure 44. Schematic of an anti-roll tank

A series of calculations were performed to determine the effectiveness of the passive anti-roll tank system in reducing the ship's susceptibility to parametric roll. Figure 45 shows the predicted maximum roll angles for the C11 containership in regular head seas as a function of encounter frequency.

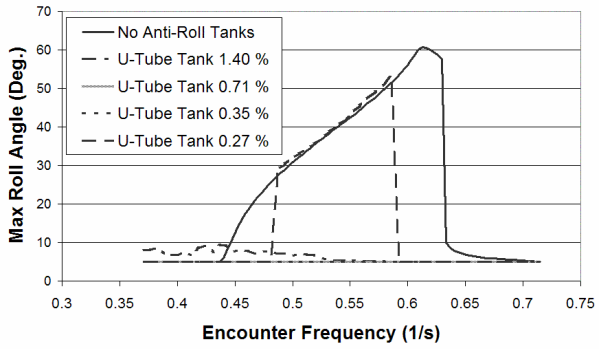

Figure 45. Parametric Roll Response with different volume of anti-roll tank

To check the performance of the U-tube tank in extreme irregular seas, simulations were made for the ship operating at various speeds and headings in a short-crested seaway. Figure 46 shows an operational polar diagram where roll motions exceed 20 degrees for the sample containership in long-crested sea state 8 conditions with a modal period of 16.4 seconds and a significant wave height of 11.49 meters.

The diagram is created from a series of LAMP simulations from 5 through 20 knots in 5-knot increments at 15-degree heading increments. All speed/heading combinations inside the shaded region exceed a 20-degree maximum roll angle during the 750-second simulation. The regions of higher speed and following seas

correspond to a resonant roll condition where the encounter frequency is near the roll natural frequency, while the head sea regions are strictly parametric roll-induced motions. The maximum roll angle for this series of simulations is 48 degrees in the head sea 10-knot case. While no simulations were performed for speeds lower than 5 knots, it should be noted that parametric roll is still possible at lower speeds. This type of diagram can be very useful in helping the shipmaster avoid the occurrence of parametric roll while the ship is operating in severe sea conditions.

The operational polar diagram shown in Figure 45 represents the LAMP predictions for the same containership fitted with an anti-roll tank system. The tank natural period is equal to the ship's roll natural period of 25 seconds, and the tank mass is equal to 0.71% of the ship's displacement. The seaway and run conditions for the simulations used to generate this figure are identical to the polar diagram in Figure 47. In contrast, this diagram shows the increased operability of this containership when a properly tuned anti-roll tank system is used.

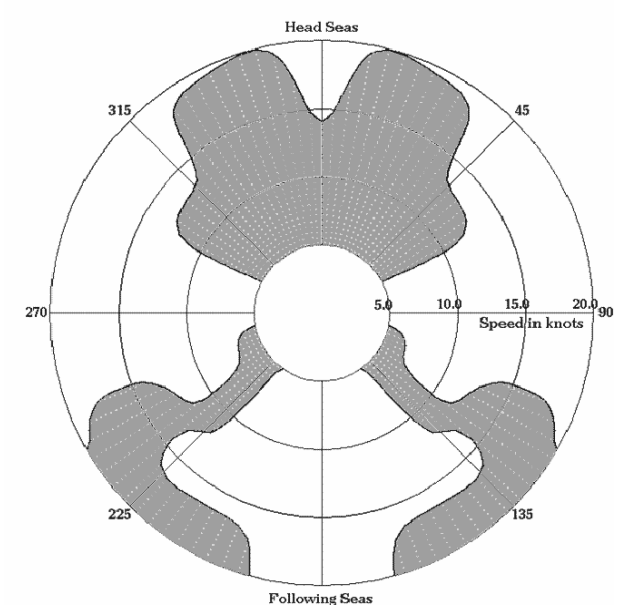

Figure 46. Polar diagram of predicted roll motion for sample containership in SS-8

The simulations used to generate the polar diagram exceeded 20 degrees of maximum roll angle in only 4 locations, corresponding to ±45 degrees at 5 knots and ±30 degrees at 20 knots head oblique seas. The maximum roll angle shown in these four simulations is less than 22 degrees, but still represents significant roll motions. The large roll motion in these four operational conditions comes about because saturation occurs in the tank system. Saturation is caused by a physical constraint on the height the fluid can move in the vertical columns, and therefore the tank system is limited in the amount of roll opposing moment that it can produce.

Overall, anti-rolling systems like the U-tube anti-roll tank appear to have a great deal of promise in the mitigation of the large roll motions caused by parametric roll. However, the optimization of such a system for maximum benefit at minimum cost will likely require a fairly sophisticated simulation system coupled to advanced probabilistic methods.

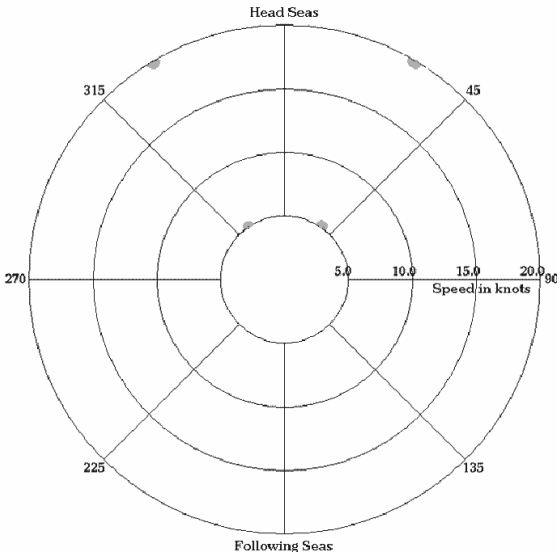

Figure 47. Polar diagram of predicted roll motion for sample containership with anti-roll tanks system

SUMMARY OF VERIFICATION OF THE GUIDE

Verification of the criteria included in the Guide [ABS 2004] was carried out for nine vessels. See Table 15. The verification procedure included:

- Calculation of GM change in wave with the Simplified method and application of the Susceptibility Criteria
- Calculation of GZ curve in wave with EUREKA and application of Severity Criteria
- LAMP Simulations in regular waves with the conditions corresponding to Severity Criteria
- LAMP Simulations in irregular waves with the variance modal period corresponding to those of the above regular.

Verification is considered to be successful if LAMP simulations reproduce parametric roll in the conditions predicted by the Guide. In Table 15, "Yes" or "No" means that susceptibility parametric roll regime was predicted or not by the Guide and correspondingly confirmed or not by LAMP simulations. The column titled "wave direction" contains information on which course the parametric roll was predicted.

The cargo ship in the last line is the same as was used in the model tests in San-Francisco Bay, where parametric roll in following seas was observed [Oakley, *et al* 1974].

Table 15 Summary of verification

Type of vessel, length and breadth in meters	Guide	Wave direction	LAMP: Regular waves	LAMP: Irregular waves
Containership L=336, B=42.8	Yes	head	Yes	Yes
Containership L=330, B=45.6	Yes	head	Yes	Yes
Containership L=262, B=40.0	Yes	head	Yes	Yes
Containership L=281, B=32.3	Yes	head	Yes	Yes
Containership L=275, B=40.0	Yes	head	Yes	Yes
Containership L=195, B=29.8	Yes	head	Yes	Yes
Tanker L=320, B=58	No	head	No	No
Bulkcarrier L=275, B=47	No	head	No	No
Cargo ship L=161, B=22.9	Yes	following	Yes	Yes

CONCLUDING REMARKS

This paper summarizes the background and results for a series of studies that have lead to the development of the ABS "Guide for the Assessment of Parametric Roll Resonance in the Design of Container Carriers" [ABS, 2004].

The paper's main focus is the development of Susceptibility Criteria that can be used to determine if there is danger of parametric roll for a particular ship. The development of these criteria is based upon the analysis of the Mathieu equation, which is the simplest mathematical model of parametric resonance. The evaluation of the resulting criteria is based principally on the evaluation of the ship's change of stability in longitudinal waves, for which a straightforward calculation method is presented. Susceptibility Criteria are complemented with the Severity Criterion which is built on the basis of a numerical solution of the roll equation in longitudinal waves and is capable of evaluation of the parametric roll amplitude.

Both criteria were verified through a series of numerical simulations using the LAMP program. To demonstrate adequacy of both criteria included in the Guide, calculations were done for nine different ships. It was found that the Guide correctly predicted the presence or absence of parametric roll for the chosen vessels.

The paper discusses some of the probabilistic aspects of numerical simulation of parametric roll in irregular waves. It is shown that in order to obtain reliable results, one realization is not enough and that distribution of the parametric roll response might be different from Gaussian.

The paper also summarizes a numerical study that has shown that U-tube passive anti-rolling might be a very effective technology to avoid the consequences of parametric resonance.

ACKNOWLEDGEMENTS

The authors wish to express their appreciation and gratitude to the management of the American Bureau of Shipping and Science Applications International Corporation.

The development of the LAMP System has been supported by the U.S. Navy, the Defense Advanced Research Projects Agency (DARPA), the U.S. Coast Guard, ABS, and SAIC. LAMP development has been supported by the Office of Naval Research (ONR) under Dr. Patrick Purtell.

REFERENCES

American Bureau of Shipping (2004). "Guide for the Assessment of Parametric Roll Resonance in the Design of Container Carriers", Houston, Texas, to be published.

Belenky, V. L. and Sevastianov, N.B. (2003). "Stability and safety of ships", Vol. 2 "Risk of capsizing", Elseveir, Amsterdam.

Belenky, V.L., Weems, K.M., W.M. Lin, and J.R. Paulling (2003). "Probabilistic analysis of roll parametric resonance in head seas" *Proc. of STAB'03 8th International Conference on Stability of Ships and Ocean Vehicles,* Madrid, Spain.

Boukhanovsky, A. V. and Degtyarev, A. B. (1996). "Nonlinear stochastic ship motion stability in different wave regime", *Proc. of CRF'96: 3rd International Conference in Commemoration of the 300-th Anniversary of Creating Russian Fleet by Peter the Great*, Vol. 2, St. Petersburg, pp. 296-306.

Bulian, G., Francescutto, A. and C. Lugni (2003). "On the nonlinear modelling of parametric rolling in regular and irregular waves", *Proc. of STAB'03 8th International Conference on Stability of Ships and Ocean Vehicles,* Madrid, Spain.

Davies, H. G. and Rajan, S. (1988). "Random superharmonic and subharmonic response: multiple time scaling of a Duffing equation", *Journal of Sound and Vibration*, Vol. 126, No 2, pp. 195-208.

Degtyarev A. B. and Boukhanovsky A.V. (2000) "Peculiarities of motions of ship with low buoyancy on asymmetrical random waves" *Proc. of STAB'2000: 7th International Conference on Stability of Ships and Ocean Vehicles,* Launceston, Australia, vol. 2, pp 665-679.

France, W.M, Levadou, M, Treakle, T.W., Paulling, J. R., Michel, K. and Moore, C. (2003). "An Investigation of Head-Sea Parametric Rolling and its Influence on Container Lashing Systems," *Marine Technology,* Vol. 40, No. 1, pp. 1-19.

Francescutto, A. and Nabergoj, R. (1990). "A stochastic analysis of nonlinear rolling in narrow band sea", *Proc. of 18th Symposium on Naval Hydrodynamics*, National Academy Press, Washington D.C.

Francescutto, A. (1991). "On the nonlinear motion of ships and structures in narrow band sea", in "Dynamics of Marine vehicles and Structure in Waves" W.G. Price, P. Temarel and A.J. Keane (editors), Elsevier Science, pp. 291-303.

Francescutto, A. (1992). "Stochastic modelling of nonlinear motions in the presence of narrow band excitation" *Proc. of the 2nd International Offshore and Polar Engineering Conference*, Vol.3, San Francisco, pp.554-558.

Francescutto, A. (1998). "On the statistical distribution of stochastic nonlinear rolling", in "*Risk and reliability in marine technology*", C. Guedes-Soares (Editor), A.A. Balkema publishers, Rotterdam, pp.107-116.

Hayashi, Ch. (1953). "Forced oscillations in non-linear systems", Nippon Printing and Publishing Company, Osaka.

Grim, O. (1961). "Beitrag zu dem Problem der Sicherheit des Schiffes im Seegang", *Schiff und Hafen*, Helft 6, pp.490-491.

IACS (2001) "Standard Wave Data", IACS Recommendation No 34, London.

Leavdou, M. and L. Palazzi (2003). "Assessment of Operational Risk of Parametric Roll", *World Maritime Conference and 2003 SNAME Annual Meeting,* San Francisco. To appear in *SNAME Transactions* Vol. 111.

Lin, W.M., and Yue, D.K.P. (1990). "Numerical Solutions for Large-Amplitude Ship Motions in the Time-Domain," *Proceedings of the Eighteenth Symposium of Naval Hydrodynamics*, The University of Michigan, U.S.A.

Lin, W.M., and Yue, D.K.P. (1993). "Time-Domain Analysis for Floating Bodies in Mild-Slope Waves of Large Amplitude," *Proceedings of the Eighth International Workshop on Water Waves and Floating Bodies*, Newfoundland, Canada.

Lin, W.M., Zhang, S., Weems, K., and Yue, D.K.P. (1999). "A Mixed Source Formulation for Nonlinear Ship-Motion and Wave-Load Simulations," *Proceedings of the Seventh International Conference on Numerical Ship Hydrodynamics*, Nantes, France.

Lin, W.M. and K. Weems (2002). "An enhanced LAMP system for high speed vessels and motion stabilization" *SAIC Report* 2002-16.

Nayfeh, A. H. (1981). "Introduction to perturbation technique", Wiley-Interscience, New York.

Neves, M., Pérez, N., Lorca, O. and C. Rodriguez (2003). "Hull design considerations for improved stability of fishing vessels in waves", *Proc. of STAB'03 8th International Conference on Stability of Ships and Ocean Vehicles,* Madrid, Spain.

Oakley, O.H., Paulling, J.R. and P.O. Wood (1974) "Ship motions and capsizing in astern seas", *Proc. of 10th Symposium on Naval Hydrodynamics*, ONR, Cambridge, Massachusetts.

Paulling J. R. and Rosenberg R.M. (1959). "On unstable ship motions resulting from nonlinear coupling", *Journal of Ship Research*, Vol. 3, No 1, pp. 36-46.

Paulling, J. R. (1961). "The transverse stability of a ship in a longitudinal seaway". *Journal of Ship Research*, vol. 4, no. 4, pp. 37-49.

Roberts, J. B. (1982). "A stochastic theory for nonlinear ship rolling in irregular seas" *Journal of Ship Research* Vol. 26, No 4, pp. 229-245.

Roberts, J. B. (1982a). "Effect of parametric excitation on ship rolling motion in random waves" *Journal of Ship Research* Vol. 26, No 4, pp. 245-253.

Sanchez, N. E. and Nayfeh, A. H. (1990). "Nonlinear rolling motions of ships in longitudinal waves", *International Shipbuilding Progress*, Vol. 37, No 411, pp.247-272.

Shin, Y.S, Belenky, V.L., Lin, W.M., Weems, K.M., Engle, A.H. (2003). "Nonlinear Time Domain Simulation Technology for Seakeeping and Wave-Load Analysis for Modern Ship Design" *World Maritime Conference and 2003 SNAME Annual Meeting,* San Francisco, To appear in *SNAME Transactions* Vol. 111.

Stoker, J. J. (1950). "Nonlinear vibrations in mechanical and electrical systems", New York.

Weems, K., Zhang, S., Lin, W.M., Shin, Y.S, and Bennett, J. (1998). "Structural Dynamic Loadings Due to Impact and Whipping," *Proceedings of the Seventh International Symposium on Practical Design of Ships and Mobile Units*, The Hague, The Netherlands.

Umeda, N. (1990). "Probabilistic study on surf-riding of a ship in irregular following seas", *Proc. of STAB'90: 4th International Conference on Stability of Ships and Ocean Vehicles*, Naples.

Umeda, N. and Yamakoshi, Ya. (1993). "Probability of ship capsizing due to pure loss of stability in irregular quartering seas", *Naval Architecture and Ocean Engineering* Vol.30, Soc. Naval Arch. Japan.

Umeda, N., Hashimoto, H., Vassalos, D., Urano, S. and K. Okou (2003). "Nonlinear dynamics on parametric roll resonance with realistic numerical modeling", *Proc. of STAB'03 8th International Conference on Stability of Ships and Ocean Vehicles,* Madrid, Spain.

Youssef, K.S., Mook, D.T., Nayfeh, A.H., and Ragab, S. A. (2003). "Roll Stabilization by Passive Anti-Roll Tanks Using an Improved Model of the Tank-Liquid Motion," submitted for publication, *J. Vibration and Control*.